Complexome Profiling Reveals Association of PPR Proteins with Ribosomes in the Mitochondria of Plants

Authors

Nils Rugen, Henryk Straube, Linda E. Franken, Hans-Peter Braun, and Holger Eubel

Correspondence

heubel@genetik.uni-hannover.de

In Brief

Plant mitochondrial protein expression is complex and routinely involves pentatricopeptide repeat proteins for processing of transcripts. Although the composition and structure of the mitoribosomes in other eukaryotic kingdoms of life is well established, plant mitochondria have so far eluded a detailed analysis. Using a complexome profiling approach, this study provides an early glimpse on the composition of plant mitochondrial ribosomes and sheds new light on the process of mitochondrial gene expression in plants. Mitochondrial subunits were found to possess several additional proteins carrying pentatricopeptide repeats potentially involved in RNA editing. Other proteins are potentially involved in the processing of nascent proteins.

Graphical Abstract
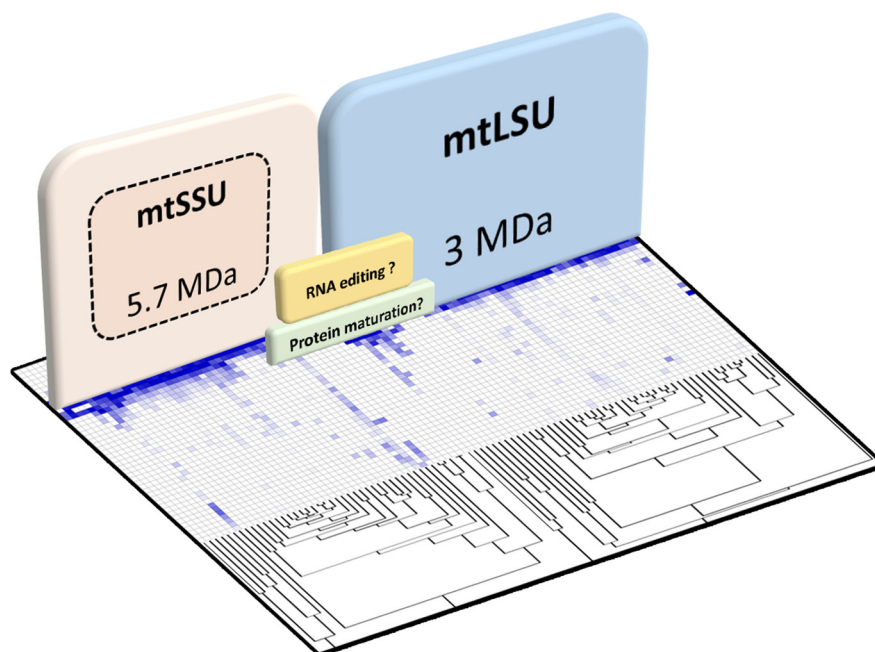
Highlights

- Plant mitoribosomes contain several pentatricopeptide repeat proteins.

- The small mitoribosomal subunit is of an exceptionally large size.

- Protein units not directly related to translation may be attached to plant mitoribosomes to confer additional functions to these molecular machines.

Complexome Profiling Reveals Association of PPR Proteins with Ribosomes in the Mitochondria of Plants⑤

Nils Rugen‡, Henryk Straube‡, ◉Linda E. Franken§¶, ◉Hans-Peter Braun‡, and ◉Holger Eubel‡¶‖

Mitochondrial transcripts are subject to a wealth of processing mechanisms including cis- and trans-splicing events, as well as base modifications (RNA editing). Hundreds of proteins are required for these processes in plant mitochondria, many of which belong to the pentatricopeptide repeat (PPR) protein superfamily. The structure, localization, and function of these proteins is only poorly understood. Here we present evidence that several PPR proteins are bound to mitoribosomes in plants. A novel complexome profiling strategy in combination with chemical crosslinking has been employed to systematically define the protein constituents of the large and the small ribosomal subunits in the mitochondria of plants. We identified more than 80 ribosomal proteins, which include several PPR proteins and other non-conventional ribosomal proteins. These findings reveal a potential coupling of transcriptional and translational events in the mitochondria of plants. Furthermore, the data indicate an extremely high molecular mass of the "small" subunit, even exceeding that of the "large" subunit. *Molecular & Cellular Proteomics 18: 1345–1362, 2019. DOI: 10.1074/mcp.RA119.001396.*

Mitochondria are semi-autonomous organelles of eukaryotic cells which produce some of their proteins using innate ribosomes (mitoribosomes). Aside from ribosomal RNA-moieties (rRNAs) and dedicated tRNAs, plant mitochondria also encode proteins involved in mRNA maturation, translation, cytochrome *c* maturation and oxidative phosphorylation (1). Several of these proteins form protein complexes which also contain subunits encoded in the nucleus. Therefore, the components of these complexes are derived from two different genomes, located in the nucleus and in the mitochondria themselves, thus defining many mitochondrial protein complexes as chimeras.

Due to their α-proteobacterial origin, mitoribosomes largely resemble bacterial 70S ribosomes with respect to their sedimentation behavior, RNA content, and susceptibility to certain antibiotics (2). They also use similar initiation and elongation factors (3, 4). However, mitoribosomes have evolved considerably in the eukaryotic lineage. Reconstruction of the mitochondrial ribosomes of the Last Eukaryotic Common Ancestor (LECA)[1] revealed that mitoribosomes were initially larger and possessed more subunits than their bacterial counterpart (5). In addition, the mitoribosomal polypeptide exit tunnel possesses a more hydrophobic surface than that of bacterial ribosomes and thus caters for the high proportion of hydrophobic respiratory chain subunits produced in mitochondria (6).

The mitoribosomes of yeast, mammals, and trypanosomes are well characterized and their respective structures have been determined at near-atomic resolution using cryo-electron microscopy (7, 8, 9). The 74S yeast mitoribosomes are composed of a 54S large subunit (mtLSU) and a 37S small subunit (mtSSU). Together, they contain 73 proteins (34 in the mtSSU, 39 in the mtLSU) and two rRNAs (15S in the mtSSU and 21S in the mtLSU). Both, the 21S rRNA of the LSU as well as the 15S rRNA of the SSU consist of more nucleotides than their *E. coli* counterparts (8, 10, 11). Yeast mitoribosomes, however, lack the 5S rRNA found in the bacterial LSU, as well as the bacterial 5S rRNA binding proteins (10).

Mammalian mitoribosomes possess a lower sedimentation coefficient of 55S and dissociate into a 28S small subunit and a 39S large subunit. Together they consist of ~80 proteins, of which 30 are present in the mtSSU and 50 in the mtLSU (12, 13, 14, 15). Limited to the synthesis of respiratory subunits, a large portion of mammalian mitoribosomes interact with the inner mitochondrial membrane (16, 17). Only containing the 16S (mtLSU) and 12S (mtSSU) rRNA, mammalian mitoribosomes also lack the 5S rRNA of the bacterial LSU, instead utilizing a mt-tRNA[Val] (18, 6). A general reduction in structural rRNA content, particularly in bridging the two subunits, is compensated for by additional proteins (19). As such, the mammalian ribosome possesses 36 proteins which are absent in its bacterial counterpart (14, 20).

The substitution of rRNA elements through the acquisition of novel ribosomal proteins, as shown for the mammalian mitoribosomes, is further perpetuated by trypanosomal mitoribosomes. Here, two extremely reduced rRNAs (9S and 12S) are joined by 127 ribosomal proteins (57 in the mtSSU and 70 in the mtLSU) in a 4.5 MDa ribonucleoprotein complex (9). A significant portion of these proteins is predicted to have functions different from those of classical ribosomal subunits. Striking features of trypanosome mitoribosomes include a small subunit of exceptionally large size and the presence of tetratricopeptide and pentatricopeptide repeat (PPR) proteins.

The latter are also present in plant mitochondria. The Arabidopsis genome encodes ~450 PPR proteins, the majority of which are predicted to be imported into mitochondria (21). While some of these proteins are involved in the processing of mitochondrial mRNAs, the functions for many mitochondrial PPR proteins are currently unknown. However, the presence of a PPR-protein in polysome fractions isolated from Arabidopsis mitochondria suggests the participation of some plant PPR proteins in mitochondrial translation (22).

Knowledge of the protein composition and structure of plant mitoribosomes is scarce. Mitoribosomes of higher plants have a sedimentation coefficient of 70–78S (depending on plant species and assay conditions) and possess 18S rRNA (mtSSU) as well as 5S and 26S rRNA (mtLSU). Furthermore, the number of proteins varies with at least 68 proteins in potato and ~80 proteins in broad bean (23–26). However, since reliable protein identification techniques such as mass spectrometry only became accessible after these studies were conducted, only a minor portion of these proteins are known. More recently, ribosomal proteins were identified as part of the plant mitochondrial proteome using shotgun and other proteomic approaches (27–31). Salvato *et al.* (30) identified more than 80 ribosomal proteins, but among these are a considerable number of cytosolic ribosomal subunits. It thus remains unclear which proteins constitute the plant mitochondrial ribosome. Due to the large extent by which mRNAs of mitochondria-encoded genes are processed, gene expression in plant mitochondria is complex and differs considerably from that of yeast and mammalian mitochondria. The sequence-specific deamination of cytosine nucleotides in mRNAs (RNA editing) is a frequently occurring process in plant mitochondria and requires a wealth of specialized RNA-binding proteins and editing factors. It is currently unclear if RNA editing occurs in the bulk phase of the mitochondrial matrix or bound to intramitochondrial structures such as mi-

toribosomes. However, analysis of eubacterial as well as cytosolic ribosomes showed that additional proteins involved in protein processing bind to the polypeptide exit tunnel (32). Additionally, yeast mitoribosomes are located in close proximity to the inner mitochondrial membrane, where they interact with proteins mediating the insertion of newly synthesized proteins into the lipid bilayer (33). As such, plant mitoribosomes can be expected to contain (or associate with) proteins not only directly involved in protein synthesis, but also in upstream steps (*i.e.* RNA processing) as well as downstream steps (*i.e.* protein processing) of translation.

Using a complexome profiling approach (34), we here report on the protein composition of plant mitochondrial ribosome subunits and subunit fragments. To this end, formaldehyde cross-linked protein complexes of plant mitochondria were first separated on either large-pore blue-native (lpBN) gels (35) or in sucrose velocity gradients. LpBN gel lanes were finely cut into >40 pieces of equal size, each of which was then analyzed in respect to protein composition and abundance by tandem mass spectrometry. Sucrose velocity gradients were fractionated into 29 fractions of equal volume and subsequently analyzed by the same method. For each separation approach, protein abundance profiles for approximately one thousand proteins were produced. Hierarchical clustering then allowed identification of proteins with similar abundance profiles. Co-migration of proteins within the gel or the sucrose velocity gradient is indicative of the presence of the proteins within the same protein complex. Our results suggest that the mtSSU has an unexpectedly large size, even surpassing that of the large subunit. Furthermore, the presence of several PPR-proteins and peptidases as well as proteases within the mitoribosomal subunits is observed, considerably extending our current knowledge on the protein composition of plant mitoribosomes.

MATERIALS AND METHODS

Mitochondria Isolation—preparation of organelles from Arabidopsis cell culture and leaf material was performed as described previously (31, 36), except for the isolation procedure for cross-linked leaf mitochondria, which involved an additional cross-linking step. Cross-linking was performed by adding 37% [v/v] formaldehyde solution to the filtered cell homogenate to a final concentration of 0.5% [v/v]. After differential and isopycnic centrifugation, as well as four washing steps to quantitatively remove Percoll from the isolated organelles, the mitochondrial concentration was adjusted to 3 mg protein/ml (according to Bradford). Only freshly prepared mitochondria were used for large pore Blue-Native PAGE and sucrose velocity gradient centrifugation.

Large Pore Blue-Native PAGE—lpBN-PAGE was carried out according to Strecker *et al.* (35) with minor modifications. To solubilize the membranes, 75 μg of protein (cell culture mitochondria, leaf mitochondria) or 125 μg protein (cross-linked leaf mitochondria) were treated by addition of 25 μl and 42 μl, respectively, of digitonin solubilization buffer (50 mM imidazole, 50 mM NaCl, 2 mM aminocaproic acid (ACA), 1 mM EDTA and 5% [w/v] digitonin, pH 7.0), and incubated for 20 min on ice. After addition of Coomassie G250 to 5% [w/v], protein complexes were loaded onto an acrylamide gradient gel

---

(2% T, 20% C to 13% T, 3% C, in 0.5 M 6-aminohexanoic acid, 25 mM imidazole/HCL, pH 7.4) overlaid with a 2.5% T, 25% C (in 0.5 M 6-aminohexanoic acid, 25 mM imidazole/HCL, pH 7.4) sample gel. After 1 h at 100 V, separation continued for another 20 h at 15 mA at max. 500 V. To stabilize the fragile high molecular-mass part of the gel, the matrix was firmly attached to one of two glass plates by binding silane (GE Healthcare, Uppsala, Sweden) whereas the opposite plate was treated with releasing agent (Blueslick, SERVA electrophoresis GmbH, Heidelberg, Germany) according to the manufacturer's directions. After Coomassie staining, the gel lane was cut into ~48 fractions from top to bottom, and each of section was subsequently subjected to in-gel trypsin digestions as outlined in (31). The procedure was modified to avoid contamination of the UPLC with remnants of soft gel pieces carried over from the peptide extraction steps (now performed in two steps, first in 50% [v/v] ACN, 2.5% [v/v] formic acid, and then in 100% [v/v] acetonitrile (ACN), 1% [v/v] formic acid).

Sucrose Velocity Gradient Separation of Protein Complexes— freshly prepared mitochondria (in suspension) were subjected to protein solubilization with digitonin as described above. The sample was subsequently layered on top of a 15 ml 8% [w/v] to 40% [w/v] sucrose gradient (in 100 mm SureSpin 630 tubes, Thermo Scientific, Bremen, Germany) and centrifuged for 6 h at 125,000 $\times$ g. After piercing the bottom of the tube with a hot needle to create a small drain hole, fractions of 500–600 μl were collected manually, resulting in 29 fractions. Of each fraction, 75 μl were then mixed with 4x Laemmli buffer (0.2 M Tris, pH 6.8; 8% [w/v] sodium dodecylsulfate (SDS); 40% [v/v] glycerol; 20% [v/v] β-mercaptoethanol; 0.2% [w/v] bromphenol blue) and loaded onto a Tris-glycin SDS gel consisting of a 4% [w/v] acrylamide stacking gel and a 14% [w/v] acrylamide separating gel as reported previously (37). The gel run was stopped when the bromphenol blue front reached the separation gel, thus leaving the proteins concentrated in a single band at the border of the two phases. Following gel fixation and Coomassie staining, the single gel bands were excised from the gel and subjected to in-gel trypsin digestion as described in Thal *et al.* (37).

Liquid Chromatography Coupled Tandem Mass Spectrometry (LC-MS/MS)—LC-MS/MS of lpBN gel fractions and sucrose velocity gradient fractions was carried out as described in (37).

Processing of MS Data—LC-MS/MS spectra were queried against a TAIR10 database additionally containing common contaminations by using the MaxQuant software version 1.6.0.1 (38). The following parameters were selected: carbamidomethyl (C) as fixed modification, oxidation (M) and acetylation (protein N-term) as variable modifications, specific digestion mode with trypsin (P) and two missed cleavage sites. A FDR of 1% was applied on the PSM and protein level. Protein groups identified as contaminants were removed manually from the proteinGroups.txt file. The data are deposited at the ProteomeXchange Consortium using the PRIDE partner repository and carry the dataset identifier PXD011088. Abundance profiles of proteins across all gel and gradient fractions (based on iBAQ values; (39)) were produced by the NOVA software (version 0.5.9.1; (40)) and subsequently clustered hierarchically using the average linkage procedure based on the Pearson correlation distance. No normalization was performed.

Experimental Design and Statistical Rationale—the heatmaps presented in this manuscript were obtained by a complexome profiling approach. For each heatmap, more than 40 readings were performed for each of the three gel-based heatmaps and 29 for the sucrose velocity gradient based heatmap. Due to the considerable protein overlap in neighboring gel slices, the results for gel slice x are confirmed by the results obtained by slice x-1 and x+1. The different heatmaps refer to independent biological experiments.

RESULTS AND DISCUSSION

Protein Correlation Profiling and Complexome Profiling— Separation of protein complexes in combination with LC-MS/MS has been successfully employed in the past to identify stable protein complexes, either of total cell extracts or of pre-purified cellular compartments, *i.e.* organelles. Most commonly, chromatographic methods or sucrose velocity gradients have been used for the separation of native complexes (41–43). In plants, this strategy has been adopted for the analysis of chloroplasts (44) and cellular extracts (45–47). Mitochondrial ribosomes in plants have so far eluded characterization by protein correlation profiling (PCP). This is most likely due to their low abundance within the organelles and the little contribution mitochondria make toward cellular protein content. In a bid to characterize low abundant plant mitochondria protein complexes, we here use electrophoretic separation of protein complexes solubilized from isolated organelles. LpBN gels enable separation of complexes with molecular masses exceeding 30 MDa (35). In contrast to chromatography-based methods, gel separation does not lead to a dilution of protein complexes in the mobile phase, which is beneficial to the subsequent LC-MS/MS analysis.

Complexome Profiling of Arabidopsis Cell Culture Mitochondria—Mitochondria prepared from a non-green Arabidopsis suspension cell culture (36) were solubilized in 2.5% digitonin and protein complexes and proteins were subsequently separated in lpBN gels. The resulting gel lane was cut into 48 horizontal fractions of equal size and subsequently subjected to LC-MS/MS analysis (31). Protein identification and quantitation in all fractions was then performed using MaxQuant (48). Across the entire 48 fractions, 1318 proteins were identified by this approach. Based on the cumulated intensity-based absolute quantitation (iBAQ) values for each protein across the 48 fractions and the putative intracellular location of the proteins as deduced from the SUBAcon algorithm (49), it can be concluded that more than 94% of the protein abundance in the mitochondrial fraction are of mitochondrial origin (see below). Cumulated iBAQ values of all proteins within each individual gel fraction also reveal a sharp drop in protein content in the fractions above 2 MDa, consistent with the low Coomassie staining intensity in this region (Suppl. Fig. 1). Interestingly, this loss of protein abundance has no negative effect on the number of protein identifications, suggesting the presence of low abundant, high molecular mass protein complexes in the upper region of the gel lane. Based on the abundance profiles of the proteins identified across all 48 gel fractions, a complexome map was built using the NOVA software (40) (supplemental Fig. S2 and S3; supplemental Table S1 and S2). The map revealed numerous protein clusters along the whole gel lane, each of which potentially representing a stable protein complex. The validity of this approach was tested against the migration pattern of respiratory complex I (NADH/ubiquinone oxidoreductase,

(supplemental Fig. S4), which has been investigated in great detail (50). In the complexome map, 50 subunits of this respiratory complex form a cluster which has a main peak at 1 MDa and an additional peak at 1.5 MDa. The 1 MDa peak corresponds to monomeric complex I, while the 1.5 MDa peak represents a supercomplex of complex I with dimeric complex III. These results are in concordance with previous investigations (31, 51). Four confirmed complex I members are not featured in the complex I cluster shown in Suppl. Fig. 4. These include NAD6 (ATMG00270), the 13 kDa protein (AT3G03070), the B18 protein (AT2G02050), and AT3G06310, a protein of unknown function. Most of these members have a local peak at either 1 MDa (NAD6, AT3G06310, B18 protein), or at 1.5 MDa (13 kDa protein, B18 protein) and are not featured in the cluster due to additional peaks (assembly/breakdown intermediates) or due to a different weighting between individual complex I and the supercomplex.

Other protein complexes with similar migration patterns, such as the prohibitin complex, which migrates close to complex I, can clearly be distinguished from complex I. Similar results are obtained for other members of the respiratory chain, indicating that complexome profiling employing lpBN-PAGE is well suited for studying the composition of protein complexes in plant mitochondria.

Complex I, together with other respiratory protein complexes, was used for a mass calibration of the map. The Arabidopsis pyruvate dehydrogenase complex served in calibrating the gel region above 1.5 MDa. In accordance with the size of this complex from mammalian mitochondria (52), its mass is set to 9 MDa. Extrapolation of the exponential graph incorporating the respiratory complexes as well as the pyruvate dehydrogenase complex (PDC) allowed calibration of the map in the >9 kDa region (supplemental Fig. S5).

Mitochondrial ribosomes were not detected in an earlier investigation employing complexome profiling which covered the molecular mass range up to 2 MDa (31). To test if ribosomal proteins are present in the >2 MDa region of the lpBN gel lane, a list of all confirmed and potential ribosomal proteins in Arabidopsis was created from literature reports (44, 53, 54), supplemented by querying The Arabidopsis Information Resource (TAIR, www.arabidopsis.org) and NCBI (www.ncbi.nlm.nih.gov) for ribosome-related annotations. The resulting list has 824 entries including structural ribosomal proteins as well as assembly factors from the cytosol, plastids, and mitochondria (supplemental Table S3). To gain a better view on potential ribosomal subclusters in cell culture mitochondria, non-ribosomal proteins were removed from the heatmap and the residual 73 ribosomal proteins were re-clustered, forming clusters of low intensity, which are mostly found in the low molecular mass region (<1 MDa) of the gel (supplemental Fig. S6). According to the SUBAcon algorithm (49), the majority of the identified ribosomal proteins (RPs) are of mitochondrial origin (60.3%), followed by cytosolic RPs (31.5%), and only a minor portion being from the plastid compartment (5,5%). No intact ribosomes nor mtSSU or mtLSU subunits were identified in this heatmap. Despite the absence of mitoribosomal subunits, the data presented in supplemental Fig. S2 do contain a wealth of information on other potential PPIs in mitochondria of non-green tissue, which may be of interest to the reader.

Complexome Profiling of Arabidopsis Leaf Mitochondria— The experimental approach described for the cell culture was also used on slower-growing leaf material. We identified 1210 proteins across the 48 fractions. Cumulated iBAQ values, calculated in the same fashion as outlined for the cell culture, show that more than 87% of the protein abundance in the mitochondrial fraction is of mitochondrial origin and that plastids/thylakoids constitute the major contamination (see below). Like the complexome map of cell culture, protein abundance in the high molecular mass region of the lpBN gel lane dropped noticeable (supplemental Fig. S7). In contrast, protein diversity in this region is even higher than in the cell culture fraction (compare supplemental Fig. S1 and S7). This is mostly due to the presence of thylakoid photosystem assemblies which cannot be removed quantitatively from mitochondrial fractions during organelle preparations from green tissue (supplemental Figs. S8 and S9; supplemental Table S4 and S5). In total, 131 of the ribosomal or ribosome-associated proteins featured in supplemental Table S3 were detected across the 48 fractions (supplemental Fig. S10). In the leaf heatmap, the abundance profiles of these proteins differ considerably from those of the cell culture. Toward the upper end of the gel lane (at ~30 MDa), a high molecular mass cluster containing 60 ribosomal proteins is visible. According to SUBAcon (49), the bulk of these proteins is located in the cytosol, while a minor fraction is of plastid origin. Owing to the high molecular mass of the cluster (the proteins were just able to enter the gel), we speculate that it contains mainly cytosolic polysomes. A second cluster running at 3 MDa contains 14 proteins of the cytosolic 60S LSU. Some of these proteins also show weak intensities at 30 MDa, indicative of their participation in the alleged cytosolic polysomes found higher up in the gel. It is currently unknown, why cytosolic polysomes should remain stable in conditions which lead to the destabilization of mitoribosomes.

Clusters containing mitochondrial ribosomes are found at 4–5 MDa (seven proteins), 1.5 MDa (twelve proteins, two of which are being assigned to plastids by SUBAcon), and at 0.2 MDa (five proteins). Other ribosomal proteins with mitochondrial location are also present in the heatmap but migrate below 0.1 MDa and are thus most likely not assembled into protein complexes. Therefore, the leaf mitochondrial heatmap is also devoid of intact mitochondrial ribosomes or ribosome subunits. However, considerably more ribosomal subunits were detected than in its cell culture counterpart. In addition, the detected interactions are also different, giving rise to assemblies of higher molecular masses.
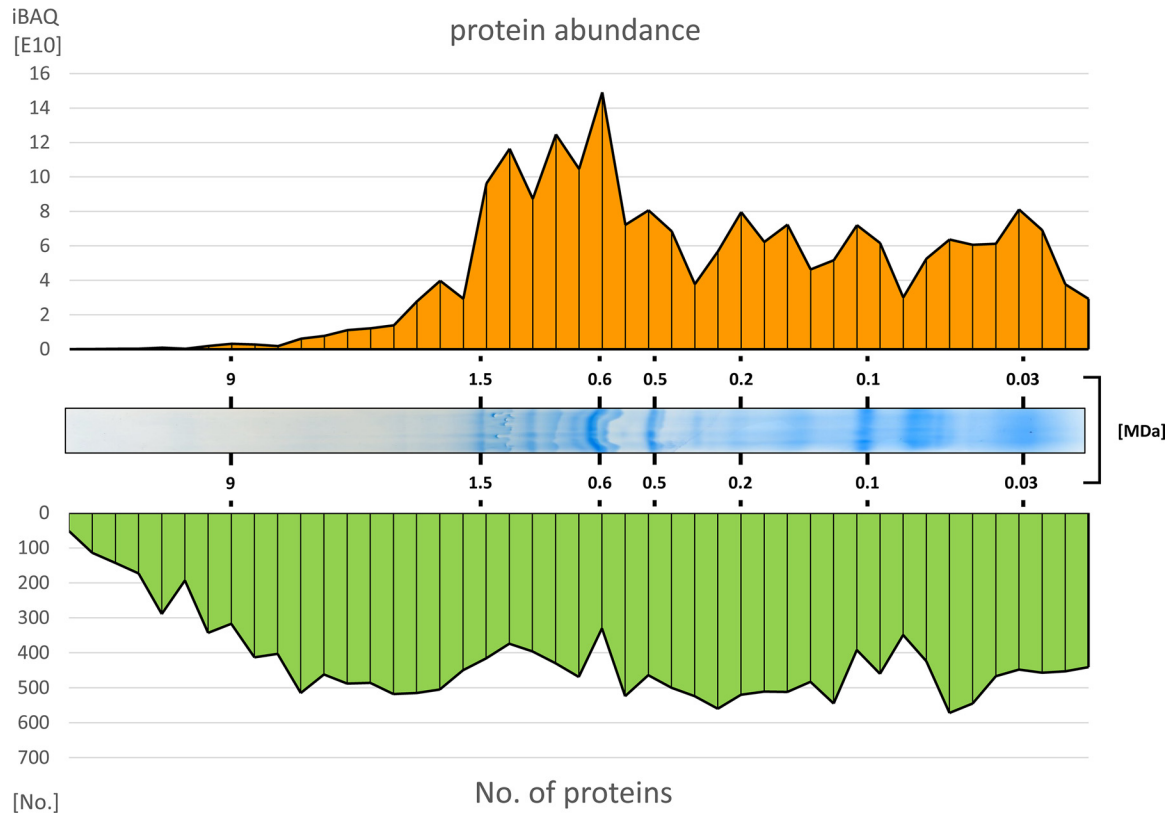
FIG. 1. **Protein abundance and protein diversity across the lpBN-PAGE of cross-linked Arabidopsis leaf mitochondria.** Digitonin solubilized leaf mitochondria were separated by lpBN-PAGE. The resulting gel lane (center panel) was cut into 48 fractions, each of which was subsequently subjected to *in gel* trypsin digestion followed by LC-MS/MS for protein identification and quantitation. Total protein abundance in each fraction (as deduced from cumulated iBAQ values) is shown in the top panel, the number of identified protein species in the bottom panel. Numbers above and below the center panel indicate molecular masses as deduced from Suppl. Fig. 5

Complexome Profiling of Cross-linked Arabidopsis Leaf Mitochondria—To improve ribosome stability, a workflow incorporating a cross-linking step early in the mitochondria isolation procedure was implemented. Protein complexes are stabilized by formaldehyde addition immediately after cell disruption, thereby freezing the state of protein complexes very shortly after ribosomal activity in the mitochondria ceases due to a lack of substrates. Complexome profiling of leaf mitochondria submitted to this experimental strategy displayed similar intensity and complexity along the gel lane when compared with its non-cross-linked counterpart (compare Fig. 1 with supplemental Fig. S7). Despite loading more protein on the gel (125 μg compared with 75 μg for not cross-linked leaf sample), the complexome map (supplemental Fig. S11 and S12; supplemental Table S6 and S7) covers less proteins (1048 compared with 1210), 77 of which are linked to ribosomes. One reason for this may be the reduced amount of plastid contamination, raising the contribution of mitochondrial proteins to more than 93% of the total protein signal. Reducing the heatmap to only the 77 ribosomal proteins, followed by re-clustering (Fig. 2) separates the bulk of the ribosomal proteins group into two clusters at ~5.7 MDa and 3.0 MDa. Less than ten predicted ribosomal proteins are

not part of either of these two complexes. Fifty-nine of the 77 proteins are of mitochondrial origin but 18 entries are assigned to the cytosol, plastids, and the plasma membrane. The non-mitochondrial ribosomal proteins largely form additional clusters and none of them is embedded in the mitoribosomal clusters. A closer look reveals that the 3.0 MDa cluster is dominated by mtLSU proteins, whereas the 5.7 MDa cluster mostly consists of mtSSU proteins. Remarkably, the large cytosolic cluster in the high molecular mass region of the non-cross-linked leaf mitochondrial heatmap is missing from this map. We conclude that 1.) formaldehyde cross-linking serves in stabilizing mitochondrial ribosomal subunits and 2.) that the mtSSU has a higher molecular mass than the mtLSU in Arabidopsis.

Other Potential Subunits in the Ribosomal Clusters of Cross-linked Arabidopsis Leaf Mitochondria—To identify novel ribosomal proteins, the master heatmap containing all identified proteins was examined for proteins co-migrating with the ribosomal proteins. Based on the Pearson correlation distance, three confidence intervals for ribosome affiliation were manually defined. Proteins with a distance value of $\leq$0.05 constitute the core of a cluster, probable candidates range between >0.05 and $\leq$0.1, and potential candidates

molecular mass [MDa]

~29   ~8   ~3   ~1   ~0.3   ~0.1

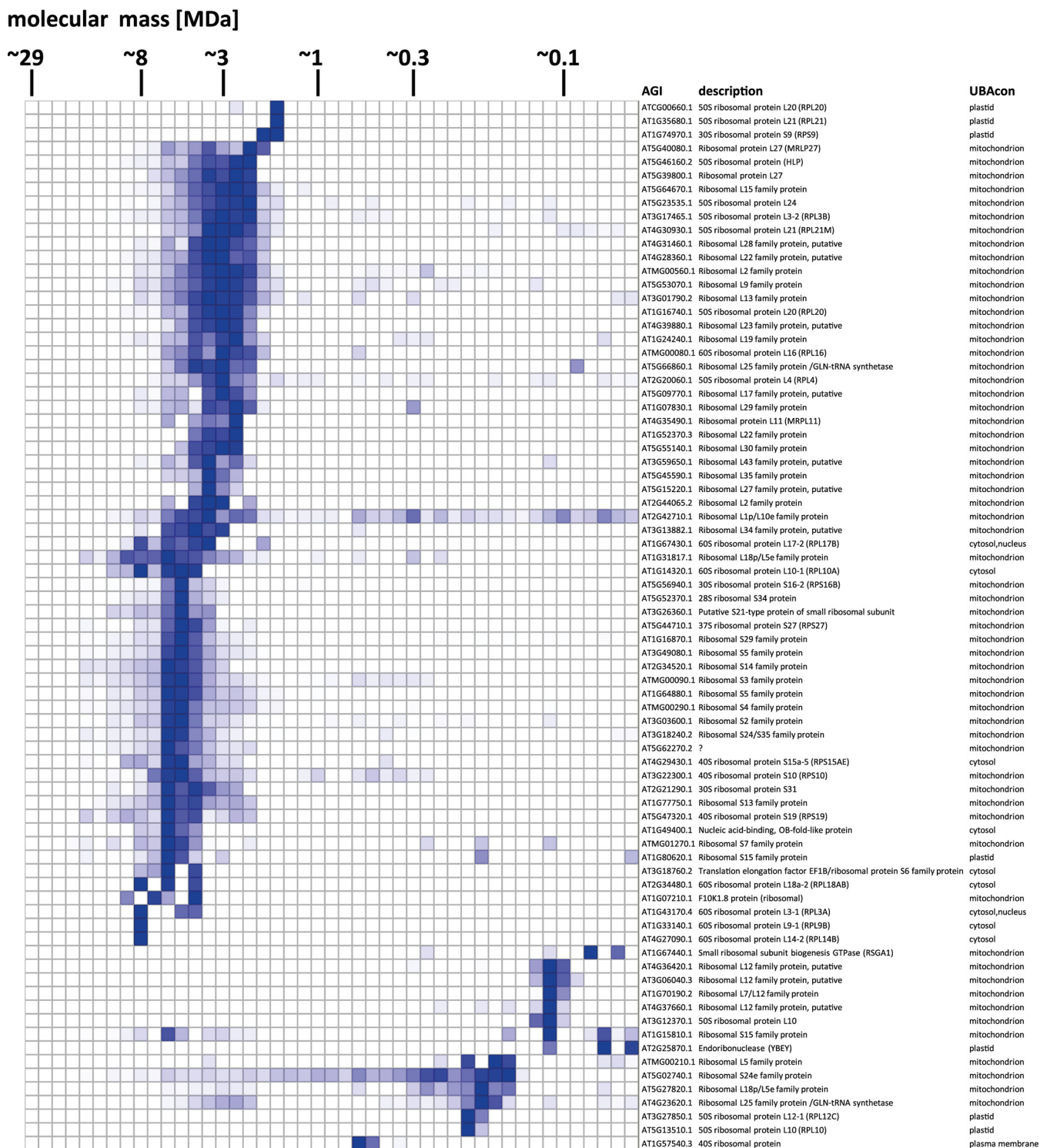| AGI	description	UBAcon
ATCG00660.1	50S ribosomal protein L20 (RPL20)	plastid
AT1G35680.1	50S ribosomal protein L21 (RPL21)	plastid
AT1G74970.1	30S ribosomal protein S9 (RPS9)	plastid
AT5G40080.1	Ribosomal protein L27 (MRLP27)	mitochondrion
AT5G46160.2	50S ribosomal protein (HLP)	mitochondrion
AT5G39800.1	Ribosomal protein L27	mitochondrion
AT5G64670.1	Ribosomal L15 family protein	mitochondrion
AT5G23535.1	50S ribosomal protein L24	mitochondrion
AT3G17465.1	50S ribosomal protein L3-2 (RPL3B)	mitochondrion
AT4G30930.1	50S ribosomal protein L21 (RPL21M)	mitochondrion
AT4G31460.1	Ribosomal L28 family protein, putative	mitochondrion
AT4G28360.1	Ribosomal L22 family protein, putative	mitochondrion
ATMG00560.1	Ribosomal L2 family protein	mitochondrion
AT5G53070.1	Ribosomal L9 family protein	mitochondrion
AT3G01790.2	Ribosomal L13 family protein	mitochondrion
AT1G16740.1	50S ribosomal protein L20 (RPL20)	mitochondrion
AT4G39880.1	Ribosomal L23 family protein, putative	mitochondrion
AT1G24240.1	Ribosomal L19 family protein	mitochondrion
ATMG00080.1	60S ribosomal protein L16 (RPL16)	mitochondrion
AT5G66860.1	Ribosomal L25 family protein /GLN-tRNA synthetase	mitochondrion
AT2G20060.1	50S ribosomal protein L4 (RPL4)	mitochondrion
AT5G09770.1	Ribosomal L17 family protein, putative	mitochondrion
AT1G07830.1	Ribosomal L29 family protein	mitochondrion
AT4G35490.1	Ribosomal protein L11 (MRPL11)	mitochondrion
AT1G52370.3	Ribosomal L22 family protein	mitochondrion
AT5G55140.1	Ribosomal L30 family protein	mitochondrion
AT3G59650.1	Ribosomal L43 family protein, putative	mitochondrion
AT5G45590.1	Ribosomal L35 family protein	mitochondrion
AT5G15220.1	Ribosomal L27 family protein, putative	mitochondrion
AT2G44065.2	Ribosomal L2 family protein	mitochondrion
AT2G42710.1	Ribosomal L1p/L10e family protein	mitochondrion
AT3G13882.1	Ribosomal L34 family protein, putative	mitochondrion
AT1G67430.1	60S ribosomal protein L17-2 (RPL17B)	cytosol,nucleus
AT1G31817.1	Ribosomal L18p/L5e family protein	mitochondrion
AT1G14320.1	60S ribosomal protein L10-1 (RPL10A)	cytosol
AT5G56940.1	30S ribosomal protein S16-2 (RPS16B)	mitochondrion
AT5G52370.1	28S ribosomal S34 protein	mitochondrion
AT3G26360.1	Putative S21-type protein of small ribosomal subunit	mitochondrion
AT5G44710.1	37S ribosomal protein S27 (RPS27)	mitochondrion
AT1G16870.1	Ribosomal S29 family protein	mitochondrion
AT3G49080.1	Ribosomal S5 family protein	mitochondrion
AT2G34520.1	Ribosomal S14 family protein	mitochondrion
ATMG00090.1	Ribosomal S3 family protein	mitochondrion
AT1G64880.1	Ribosomal S5 family protein	mitochondrion
ATMG00290.1	Ribosomal S4 family protein	mitochondrion
AT3G03600.1	Ribosomal S2 family protein	mitochondrion
AT3G18240.2	Ribosomal S24/S35 family protein	mitochondrion
AT5G62270.2	?	mitochondrion
AT4G29430.1	40S ribosomal protein S15a-5 (RPS15AE)	cytosol
AT3G22300.1	40S ribosomal protein S10 (RPS10)	mitochondrion
AT2G21290.1	30S ribosomal protein S31	mitochondrion
AT1G77750.1	Ribosomal S13 family protein	mitochondrion
AT5G47320.1	40S ribosomal protein S19 (RPS19)	mitochondrion
AT1G49400.1	Nucleic acid-binding, OB-fold-like protein	cytosol
ATMG01270.1	Ribosomal S7 family protein	mitochondrion
AT1G80620.1	Ribosomal S15 family protein	plastid
AT3G18760.2	Translation elongation factor EF1B/ribosomal protein S6 family protein	cytosol
AT2G34480.1	60S ribosomal protein L18a-2 (RPL18AB)	cytosol
AT1G07210.1	F10K1.8 protein (ribosomal)	mitochondrion
AT1G43170.4	60S ribosomal protein L3-1 (RPL3A)	cytosol,nucleus
AT1G33140.1	60S ribosomal protein L9-1 (RPL9B)	cytosol
AT4G27090.1	60S ribosomal protein L14-2 (RPL14B)	cytosol
AT1G67440.1	Small ribosomal subunit biogenesis GTPase (RSGA1)	mitochondrion
AT4G36420.1	Ribosomal L12 family protein, putative	mitochondrion
AT3G06040.3	Ribosomal L12 family protein, putative	mitochondrion
AT1G70190.2	Ribosomal L7/L12 family protein	mitochondrion
AT4G37660.1	Ribosomal L12 family protein, putative	mitochondrion
AT3G12370.1	50S ribosomal protein L10	mitochondrion
AT1G15810.1	Ribosomal S15 family protein	mitochondrion
AT2G25870.1	Endoribonuclease (YBEY)	plastid
ATMG00210.1	Ribosomal L5 family protein	mitochondrion
AT5G02740.1	Ribosomal S24e family protein	mitochondrion
AT5G22820.1	Ribosomal L18p/L5e family protein	mitochondrion
AT4G23620.1	Ribosomal L25 family protein /GLN-tRNA synthetase	mitochondrion
AT3G27850.1	50S ribosomal protein L12-1 (RPL12C)	plastid
AT5G13510.1	50S ribosomal protein L10 (RPL10)	plastid
AT1G57540.3	40S ribosomal protein	plasma membrane

FIG. 2. **Abundance profiles of ribosomal and ribosome-related proteins in cross-linked Arabidopsis leaf mitochondria.** Proteins of a mitochondrial fraction isolated from leaf material treated with formaldehyde immediately after cell disruption were separated by lpBN PAGE. The resulting gel lane was cut into 45 fractions and all fractions were subjected to label-free quantitative shotgun proteomics. The heatmap displays the abundance profiles of all potential mitoribosomal proteins detected in this approach (see Suppl. Table 3 for a list of all ribosomal and ribosome-associated proteins in Arabidopsis thaliana). Protein abundance is illustrated by color: white is absence of detection, shades of blue indicate quantities relative to the highest detected abundance (dark blue) of a particular protein across all fractions. Values on top of the heatmap indicate molecular mass as deduced from Suppl. Fig. 5. AGI, Arabidopsis genome identifier. A high resolution, interactive version of this figure enabling protein searches is found at http://complexomemap.de/ribo_fig2.
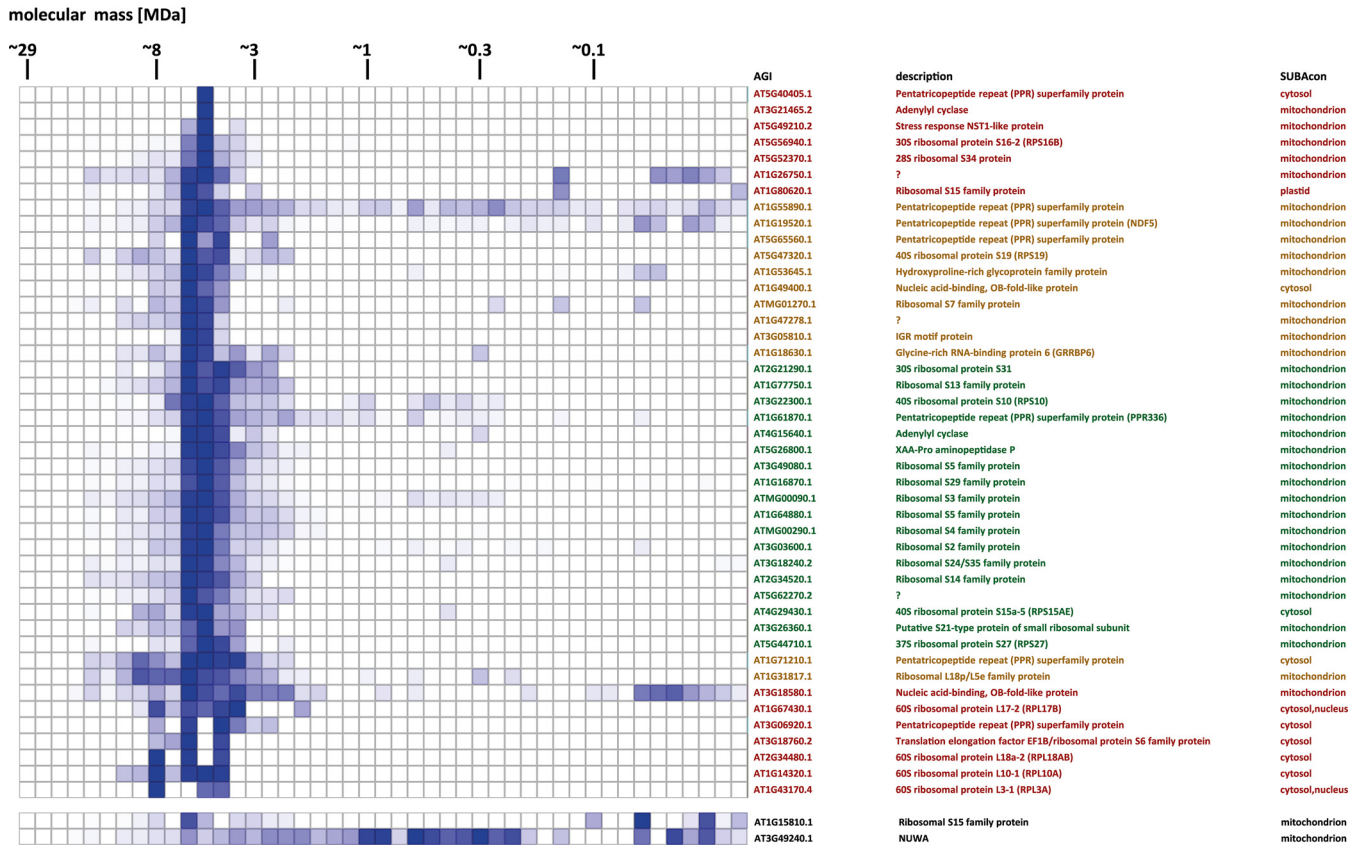
FIG. 3. **Abundance profiles of small subunit ribosomal proteins and associated proteins in cross-linked Arabidopsis leaf mitochondria.** Cutaway of the ribosomal cluster from the master heatmap (see Suppl. Fig. 11) containing small subunit ribosomal proteins and potentially associated proteins displaying similar migration patterns. Protein abundance is illustrated by color: white is absence of detection, shades of blue indicate amounts relative to the highest detected abundance of a particular protein across all fractions (dark blue). Depending on Pearson correlation distance, proteins are grouped into three classes: core proteins (green) ≤ 0.05; probable (orange) >0.05, ≤ 0.1; and potential (red) >0.1, ≤ 0.2. Ribosomal proteins found to co-migrate with the mtSSU cluster in Fig. 2, but are missing in the master heatmap cluster are shown at the bottom. AGI Arabidopsis genome identifier; SUBAcon, subcellular protein location according to the SUBAcon algorithm (Hooper *et al.* 2014). Offset heatmap row shows distribution of RPL32, which is not part of the cluster in the master heatmap but displays a migration pattern similar to other mtSSU members (see also Fig. 2). A high resolution, interactive version of this figure enabling protein searches is found at http://complexomemap.de/ribo_fig3.

have values between >0.1 and ≤0.2. The mtSSU contains 44 proteins across all three confidence intervals. Eighteen proteins are found in the core cluster while the residual 26 proteins are evenly distributed over the two remaining confidence intervals (twelve probable proteins and 14 potential proteins). Together, the two groups with lower confidence contain eleven proteins annotated as being ribosomal members and six proteins containing PPR motifs. In addition to the single PPR-protein found in the core cluster, this amounts to seven PPR-motif containing proteins in the small subunit (Fig. 3).

The mtLSU cluster consists of 48 proteins. Twenty are found in the core cluster, 17 are probable members, and eleven are potential members (Fig. 4). Like the mtSSU cluster, the bulk of the proteins are ribosomal proteins and PPR family members, but a higher diversity in respect to their functions is evident. A potential mtLSU subcluster (consisting of probable members) does not exactly match the pattern of the core

proteins and migrates somewhat below the center of the core proteins. This subcluster contains four protease/peptidase related proteins (FTSH3, FTSH10, two S24/26 peptidases) together with stomatin-like proteins 1 and 2 (SLP1, 2), as well as a PPR-protein and a protein of unknown function.

Sucrose Velocity Gradient Centrifugation of Mitoribosomal Subunits—To test if the low electrophoretic mobility of the cross-linked small mitoribosomal subunit in lpBN gels may be related to the electrophoretic conditions, digitonin-solubilized protein complexes of cross-linked leaf mitochondria were separated in an 8% to 40% sucrose gradient. After 80 min of ultracentrifugation, the gradient was fractionated into 29 fractions of ~500 μl each, which were subsequently subjected to LC-MS/MS analysis. From this, a heatmap was built in the same fashion as described for the gel fractions (supplemental Fig. S13 and S14, supplemental Table S8 and S9). In total, 919 proteins were identified across the 29 fractions. Hierarchical clustering revealed two broad ribosomal clusters. Using
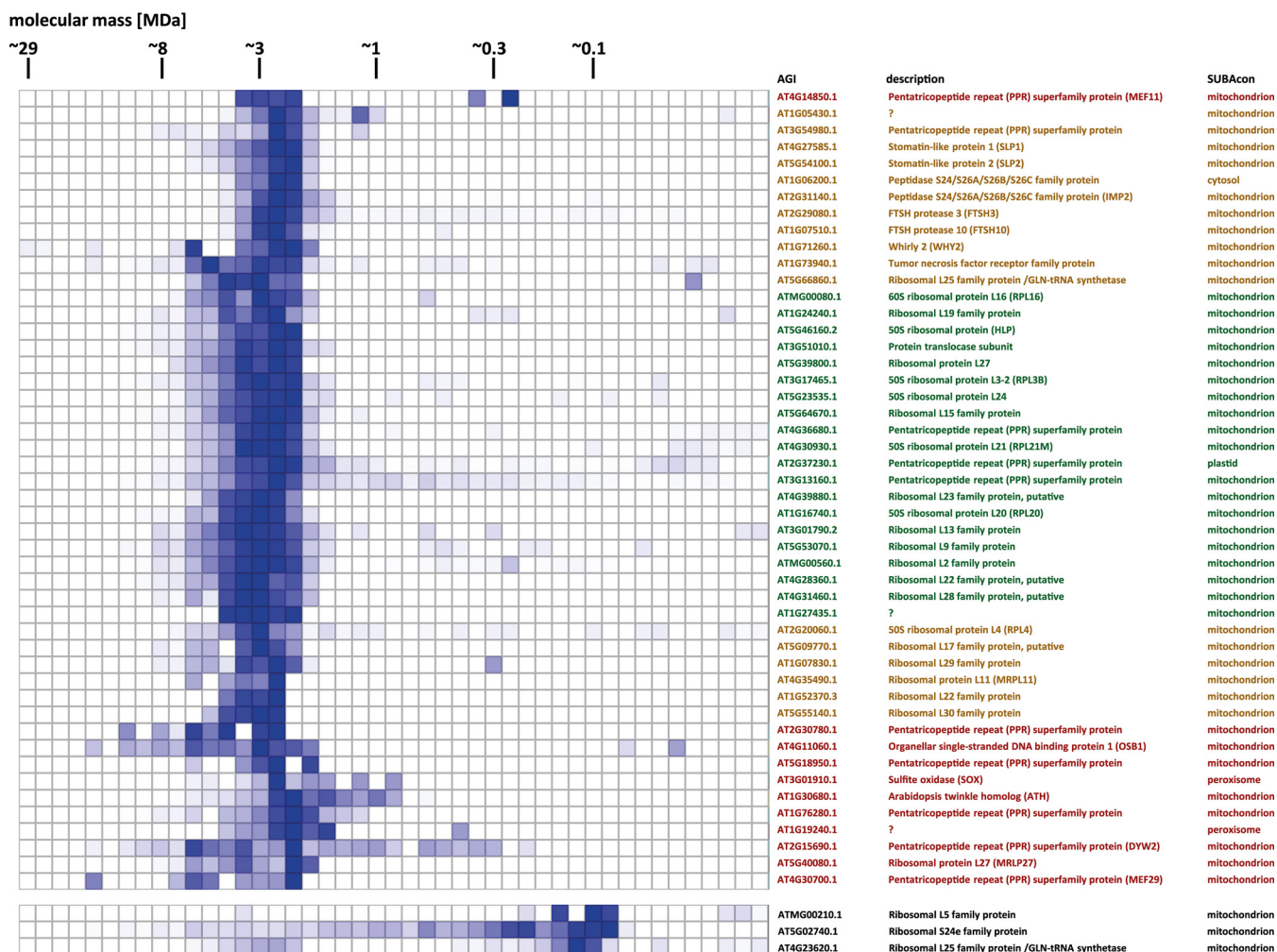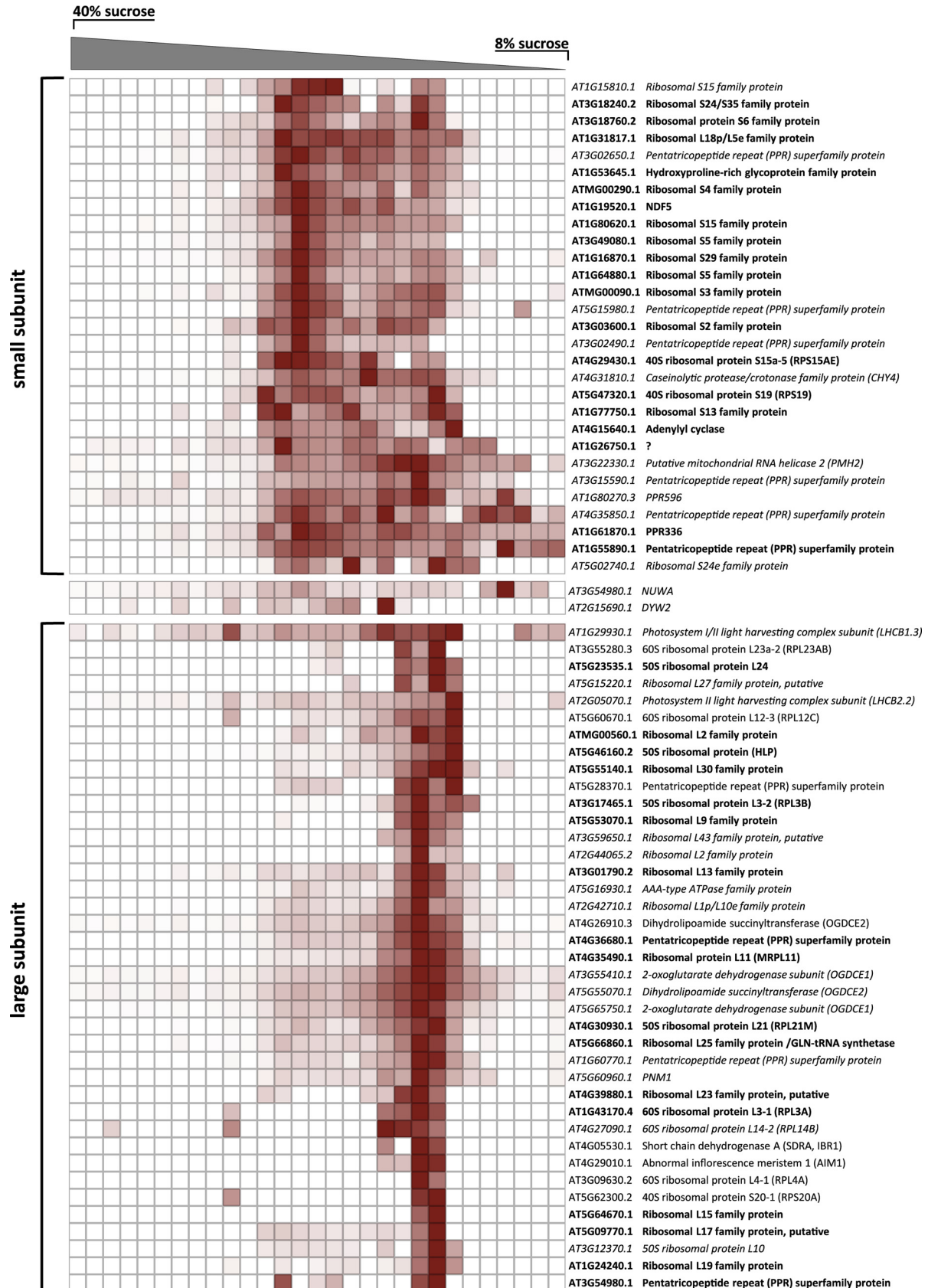
FIG. 4. **Abundance profiles of large subunit ribosomal proteins and associated proteins in cross-linked Arabidopsis leaf mitochondria.** Cutaway of the ribosomal cluster from the master heatmap (see Suppl. Fig. 11) containing large subunit ribosomal proteins and potentially associated proteins displaying similar migration patterns. Protein abundance is illustrated by color: white is absence of detection, shades of blue indicate amounts relative to the highest detected abundance of a particular protein across all fractions (dark blue). Proteins are grouped into three classes, depending on Pearson correlation distance: core proteins (green) ≤ 0.05; probable (orange) >0.05, ≤0.1; and potential (red) >0.1, ≤0.2. Ribosomal proteins found to co-migrate with the mtLSU cluster in Fig. 2 but missing in the master heatmap cluster are shown at the bottom. AGI, Arabidopsis genome identifier; SUBAcon, subcellular protein location according to the SUBAcon algorithm (Hooper *et al.* 2014). Offset heatmap rows show distribution of other mtLSU members, which are not part of the cluster in the master heatmap but display similar migration patterns (see also Fig. 2). A high resolution, interactive version of this figure enabling protein searches is found at http://complexomemap.de/ribo_fig4.

a Pearson correlation distance cutoff of 0.2, they contained 29 mtSSU and 39 mtLSU proteins (Fig. 5). Of these, 19 and 17 proteins, respectively, were also found in the two ribosomal clusters of lpBN PAGE separated cross-linked leaf mitochondria. Separation of protein complexes within the sucrose velocity gradient is inferior to that within the gel matrix of the lpBN PAGE, as indicated by the increased width of the clusters and the presence of obvious non-ribosomal proteins such as 2-oxoglutarate dehydrogenase complex (OGDC) subunits among the mtLSU cluster. Nevertheless, the comparison between sucrose velocity gradient and lpBN PAGE reveals two important aspects of mitoribosomes in plants. First, loosely attached subunits may be lost from protein complexes during

lpBN PAGE as indicated by the presence of additional ribosomal proteins and PPR proteins within the ribosomal clusters of the sucrose velocity gradient. Vice versa, some proteins present in the lpBN clusters are absent from the mitoribosomal clusters in the sucrose velocity gradient. This may be due to either a different migration pattern (indicating the absence of this protein from the respective ribosomal subunit), or to the low resolution in the sucrose velocity gradient heatmap hampering hierarchical clustering. Second, the small mitoribosomal subunit migrates of a position in the sucrose velocity gradient that indicates a higher molecular mass when compared with the large subunit. Thus, the results obtained by sucrose velocity gradient separation confirm the relative

40% sucrose

8% sucrose

small subunit

AT1G15810.1 *Ribosomal S15 family protein*
AT3G18240.2 **Ribosomal S24/S35 family protein**
AT3G18760.2 **Ribosomal protein S6 family protein**
AT1G31817.1 **Ribosomal L18p/L5e family protein**
AT3G02650.1 *Pentatricopeptide repeat (PPR) superfamily protein*
AT1G53645.1 **Hydroxyproline-rich glycoprotein family protein**
ATMG00290.1 **Ribosomal S4 family protein**
AT1G19520.1 **NDF5**
AT1G80620.1 **Ribosomal S15 family protein**
AT3G49080.1 **Ribosomal S5 family protein**
AT1G16870.1 **Ribosomal S29 family protein**
AT1G64880.1 **Ribosomal S5 family protein**
ATMG00090.1 **Ribosomal S3 family protein**
AT5G15980.1 *Pentatricopeptide repeat (PPR) superfamily protein*
AT3G03600.1 **Ribosomal S2 family protein**
AT3G02490.1 *Pentatricopeptide repeat (PPR) superfamily protein*
AT4G29430.1 **40S ribosomal protein S15a-5 (RPS15AE)**
AT4G31810.1 *Caseinolytic protease/crotonase family protein (CHY4)*
AT5G47320.1 **40S ribosomal protein S19 (RPS19)**
AT1G77750.1 **Ribosomal S13 family protein**
AT4G15640.1 **Adenylyl cyclase**
AT1G26750.1 **?**
AT3G22330.1 *Putative mitochondrial RNA helicase 2 (PMH2)*
AT3G15590.1 *Pentatricopeptide repeat (PPR) superfamily protein*
AT1G80270.3 *PPR596*
AT4G35850.1 *Pentatricopeptide repeat (PPR) superfamily protein*
AT1G61870.1 **PPR336**
AT1G55890.1 **Pentatricopeptide repeat (PPR) superfamily protein**
AT5G02740.1 *Ribosomal S24e family protein*

AT3G54980.1 *NUWA*
AT2G15690.1 *DYW2*

large subunit

AT1G29930.1 *Photosystem I/II light harvesting complex subunit (LHCB1.3)*
AT3G55280.3 60S ribosomal protein L23a-2 (RPL23AB)
AT5G23535.1 **50S ribosomal protein L24**
AT5G15220.1 *Ribosomal L27 family protein, putative*
AT2G05070.1 *Photosystem II light harvesting complex subunit (LHCB2.2)*
AT5G60670.1 60S ribosomal protein L12-3 (RPL12C)
ATMG00560.1 **Ribosomal L2 family protein**
AT5G46160.2 **50S ribosomal protein (HLP)**
AT5G55140.1 **Ribosomal L30 family protein**
AT5G28370.1 *Pentatricopeptide repeat (PPR) superfamily protein*
AT3G17465.1 **50S ribosomal protein L3-2 (RPL3B)**
AT5G53070.1 **Ribosomal L9 family protein**
AT3G59650.1 *Ribosomal L43 family protein, putative*
AT2G44065.2 *Ribosomal L2 family protein*
AT3G01790.2 **Ribosomal L13 family protein**
AT5G16930.1 *AAA-type ATPase family protein*
AT2G42710.1 *Ribosomal L1p/L10e family protein*
AT4G26910.3 Dihydrolipoamide succinyltransferase (OGDCE2)
AT4G36680.1 **Pentatricopeptide repeat (PPR) superfamily protein**
AT4G35490.1 **Ribosomal protein L11 (MRPL11)**
AT3G55410.1 *2-oxoglutarate dehydrogenase subunit (OGDCE1)*
AT5G55070.1 *Dihydrolipoamide succinyltransferase (OGDCE2)*
AT5G65750.1 *2-oxoglutarate dehydrogenase subunit (OGDCE1)*
AT4G30930.1 **50S ribosomal protein L21 (RPL21M)**
AT5G66860.1 **Ribosomal L25 family protein /GLN-tRNA synthetase**
AT1G60770.1 *Pentatricopeptide repeat (PPR) superfamily protein*
AT5G60960.1 *PNM1*
AT4G39880.1 **Ribosomal L23 family protein, putative**
AT1G43170.4 **60S ribosomal protein L3-1 (RPL3A)**
AT4G27090.1 *60S ribosomal protein L14-2 (RPL14B)*
AT4G05530.1 Short chain dehydrogenase A (SDRA, IBR1)
AT4G29010.1 Abnormal inflorescence meristem 1 (AIM1)
AT3G09630.2 60S ribosomal protein L4-1 (RPL4A)
AT5G62300.2 40S ribosomal protein S20-1 (RPS20A)
AT5G64670.1 **Ribosomal L15 family protein**
AT5G09770.1 **Ribosomal L17 family protein, putative**
AT3G12370.1 *50S ribosomal protein L10*
AT1G24240.1 **Ribosomal L19 family protein**
AT3G54980.1 **Pentatricopeptide repeat (PPR) superfamily protein**

molecular masses of the plant mitoribosomal subunits and rule out an artificial, electrophoresis-related cause for the apparent molecular mass of the mtSSU in the gel-based complexome profiling approach.

Organelle Purity and Ribosome Contaminations from Other Cellular Compartments—Some of the proteins found in the four heatmaps are clearly of non-mitochondrial origin. The presence of these proteins suggest co-purification of other cellular components with the mitochondria during organelle isolation. The level of non-mitochondrial contamination within the fractions used to build the heatmaps positively correlates with the likelihood of identifying false-positive cytosolic and plastid ribosomal subunits as part of the mitochondrial ribosome. To test the purity of the mitochondrial isolates, the subcellular location of each protein was deduced by the SUBAcon algorithm. Subsequently, the cumulative abundance of each protein across the gel fractions was calculated and the resulting sums for all proteins located in the same compartment were added up. From this, relative protein abundance for each organelle was calculated (supplemental Fig. S15). Cytosolic proteins amount to ~1% in each of the four heatmaps. Contaminations of plastid proteins are generally higher, reaching 8% in the non-cross-linked leaf sample. This value is reduced to 4.3% in the cross-linked leaf sample containing the ribosomal clusters. Proteins of all other compartments amount to less than 4%. This shows that contamination of cytosolic as well as plastid proteins is low in the mitochondrial isolates used in this study. Considering that the most abundant plastid proteins are inserted into the thylakoid membranes, the likelihood of contamination of the mitochondrial ribosomes by those of plastids is judged to be very low. In contrast, a portion of the cytosolic ribosomes are attached to the mitochondrial surface (55). As such, proteins of cytosolic ribosomes may be present in mitochondrial samples despite the low abundance of cytosolic proteins in the mitochondrial isolates. Indeed, some cytosolic proteins (as described by (56)) are found in our cross-linked leaf dataset and their presence within the ribosomal clusters should be treated with caution.

The Protein Composition of the Arabidopsis Mitoribosomes—During the review-process of this manuscript, Waltz *et al.* (57) published an independent investigation of the mitochondrial ribosomes of Arabidopsis. Using two complementary approaches (epitope tagging and sucrose velocity gradient centrifugation), 94 proteins were identified as being part of the two mitoribosomal subunits in Arabidopsis flowers and a cell culture, in contrast to the 92 proteins reported here. A direct comparison of the results obtained by Waltz *et al.* (57) and those within the mtSSU and mtLSU clusters of the lpBN separated cross-linked leaf mitochondria presented here reveals an overlap of 62 proteins (66% of the 94 proteins reported by Waltz *et al.* (57), Table I). Each study also reports potential ribosomal subunit members, which are not confirmed by the other one (32 in Waltz *et al.* (57), 30 here). Within the set of the 32 Waltz *et al.* (57) specific proteins, 12 proteins were found in our complexome map to possess a second peak in the region of the mtSSU or mtLSU (indicated by the absence of a confidence interval suffix in the "lpBN PAGE" column in Table 1). These proteins are thus most likely mitochondrial riboproteins and the overlap between both data sets increases to 74 proteins (79% of the 94 proteins described by Waltz *et al.* (57)). Within the set of 74 overlapping proteins, assignment to either the mtSSU or the mtLSU is similar for all but one protein (AT3G13160, PPR superfamily protein).

The remaining 20 proteins described by Waltz *et al.* (57) were not found in the lpBN-based complexome profiling analysis. Only five of these proteins belong to the SSU. Among them are three ribosomal proteins (AT2G19720, AT4G22460, and ATMG00980) which are most likely located in mitochondria and can therefore be considered as *bona fide* mitoribosomal proteins. The remaining two SSU proteins not found by us are either of unknown function (AT1g64600) or are annotated as tyrosine sulfotransferase-like protein (At4G22000). For both proteins, experimental evidence for a mitochondrial location is missing. The majority (15 accessions) of the proteins exclusively found by Waltz *et al.* (57) are described as LSU proteins. Thirteen of the missing LSU proteins are annotated as ribosomal components and are most likely located in mitochondria. The non-ribosomal proteins include a copper ion-binding protein (AT4G05400) of unknown function and a P-class PPR protein. Both have previously been found in LC-MS/MS analyses of isolated Arabidopsis mitochondria. As such, most of the SSU and LSU proteins reported by Waltz *et al.* (57) which are missing in our clusters can be considered true mitochondrial riboproteins.

Among our list of 92 proteins which are associated with the mtSSU or mtLSU cluster in the lpBN heatmap, 30 have not been reported by Waltz *et al.* (57). Among these are ten

Fig. 5. **Abundance profiles of small and large ribosomal subunits separated by sucrose density gradient ultracentrifugation.** Digitonin-solubilized mitochondrial proteins were separated in an 8% to 40% sucrose gradient, which was subsequently fractionated. Each fraction was then subjected to LC-MS/MS and results were used to produce a heatmap in the same fashion as outlined for the lpBN PAGE (see Suppl. Figs. 2, 8, 11). Cutouts of the clusters of small (top panel) and large (bottom panel) subunits are shown. Protein abundance is illustrated by color: white is absence of detection, shades of brown indicate amounts relative to the highest detected abundance of a particular protein across all fractions. Protein names written in bold font indicate proteins which are part of the ribosomal clusters in the lpBN based heatmaps, while those written in italics represent proteins that are present in the lpBN heatmaps but are not part of the mtLSU or mtSSU clusters (Figs. 3 and 4). Please note: MS analysis of fraction 15 was hampered for unknown reasons. Protein intensities of this fraction were therefore given as the average of its two neighboring fractions. A high resolution, interactive version of this figure enabling protein searches is found at http://complexomemap.de/ribo_fig5.

TABLE I

Unified list of ribosomes as described by Waltz et al. (57) and this study

AGI	description	lpBN PAGE (Rugen)	SVC (Rugen)	Waltz	SUBAcon	GFP	MS	cytosolic ribosome	plastid ribosome
1.) components featured in Waltz et al. and lpBN ribosome clusters of Rugen et al.									
AT3G13160	rPPR3b (P-class)	mtLSU (core)	other	mtSSU	mitochondrion	+	+	-	-
AT3G26360	putative S21-type protein of small ribosomal subunit	mtSSU (core)	-	mtSSU	mitochondrion	-	-	-	-
AT2G21290	30S ribosomal protein S31	mtSSU (core)	-	mtSSU	mitochondrion	-	-	-	-
AT2G34520	ribosomal S14 family protein	mtSSU (core)	-	mtSSU	mitochondrion	-	-	-	-
AT5G44710	37S ribosomal protein S27 (RPS27)	mtSSU (core)	-	mtSSU	mitochondrion	-	+	-	-
AT5G26800	XAA-Pro aminopeptidase P	mtSSU (core)	-	mtSSU	mitochondrion	-	-	-	-
AT1G77750	ribosomal S13 family protein	mtSSU (core)	mtSSU	mtSSU	mitochondrion	+	+	-	-
AT3G03600	ribosomal S2 family protein	mtSSU (core)	mtSSU	mtSSU	mitochondrion	-	+	-	-
ATMG00290	ribosomal S4 family protein	mtSSU (core)	mtSSU	mtSSU	mitochondrion	-	+	-	-
AT1G64880	ribosomal S5 family protein	mtSSU (core)	mtSSU	mtSSU	mitochondrion	-	+	-	-
AT4G29430	40S ribosomal protein S15a-5 (RPS15AE)	mtSSU (core)	mtSSU	mtSSU	cytosol	-	+	+	-
AT3G49080	ribosomal S5 family protein	mtSSU (core)	mtSSU	mtSSU	mitochondrion	-	+	-	-
AT1G16870	ribosomal S29 family protein	mtSSU (core)	mtSSU	mtSSU	mitochondrion	-	+	-	-
AT3G18240	ribosomal S24/S35 family protein	mtSSU (core)	mtSSU	mtSSU	mitochondrion	-	+	-	-
AT1G61870	PPR336/rPPR1 (P-class)	mtSSU (core)	mtSSU	mtSSU	mitochondrion	+	+	-	-
AT4G15640	adenylyl cyclase	mtSSU (core)	mtSSU	mtSSU	mitochondrion	+	+	-	-
AT3G22300	40S ribosomal protein S10 (RPS10)	mtSSU (core)	other	mtSSU	mitochondrion	-	+	-	-
ATMG00090	ribosomal S3 family protein	mtSSU (core)	mtSSU	mtSSU	mitochondrion	-	+	-	-
AT5G62270	?	mtSSU (core)	other	mtSSU	mitochondrion	-	+	-	-
AT5G56940	30S ribosomal protein S16-2 (RPS16B)	mtSSU (pot.)	-	mtSSU	mitochondrion	+	+	-	-
AT3G21465	adenylyl cyclase	mtSSU (pot.)	-	mtSSU	mitochondrion	-	+	-	-
AT3G18760	translation elongation factor EF1B/rib. S6 family protein	mtSSU (pot.)	mtSSU	mtSSU	cytosol	-	+	-	-
AT1G80620	ribosomal S15 family protein	mtSSU (pot.)	mtSSU	mtSSU	plastid	-	+	-	-
AT1G26750	?	mtSSU (pot.)	mtSSU	mtSSU	mitochondrion	-	+	-	-
AT5G52370	28S ribosomal S34 protein	mtSSU (pot.)	other	mtSSU	mitochondrion	-	-	-	-
AT1G49400	nucleic acid-binding, OB-fold-like protein	mtSSU (prob.)	-	mtSSU	cytosol	-	-	-	-
AT1G47278	?	mtSSU (prob.)	-	mtSSU	mitochondrion	-	+	-	-
AT1G31817	ribosomal L18p/L5e family protein	mtSSU (prob.)	mtSSU	mtSSU	mitochondrion	-	+	-	-
AT5G47320	40S ribosomal protein S19 (RPS19)	mtSSU (prob.)	mtSSU	mtSSU	mitochondrion	-	+	-	-
AT1G19520	NFD5/rPPR2 (P-class)	mtSSU (prob.)	mtSSU	mtSSU	mitochondrion	-	+	-	-
AT1G55890	rPPR3a (P-class)	mtSSU (prob.)	mtSSU	mtSSU	mitochondrion	-	+	-	-
AT1G53645	hydroxyproline-rich glycoprotein family protein	mtSSU (prob.)	mtSSU	mtSSU	mitochondrion	-	+	-	-
ATMG01270	ribosomal S7 family protein	mtSSU (prob.)	other	mtSSU	mitochondrion	-	+	-	-
AT1G18630	glycine-rich RNA-binding protein 6 (GRRBP6)	mtSSU (prob.)	other	mtSSU	mitochondrion	-	+	-	-
AT1G16740	50S ribosomal protein L20 (RPL20)	mtLSU (core)	-	mtLSU	mitochondrion	-	+	-	-
AT1G27435	?	mtLSU (core)	-	mtLSU	mitochondrion	-	+	-	-
AT3G51010	protein translocase subunit	mtLSU (core)	-	mtLSU	mitochondrion	-	+	-	-
AT5G39800	ribosomal protein L27	mtLSU (core)	-	mtLSU	mitochondrion	-	+	-	-
ATMG00080	60S ribosomal protein L16 (RPL16)	mtLSU (core)	-	mtLSU	mitochondrion	-	+	-	-
AT1G24240	ribosomal L19 family protein	mtLSU (core)	mtLSU	mtLSU	mitochondrion	-	+	-	-
AT4G30930	50S ribosomal protein L21 (RPL21M)	mtLSU (core)	mtLSU	mtLSU	mitochondrion	+	+	-	-
AT5G53070	ribosomal L9 family protein	mtLSU (core)	mtLSU	mtLSU	mitochondrion	-	+	-	-
AT4G36680	rPPR7 (P-class)	mtLSU (core)	mtLSU	mtLSU	mitochondrion	-	+	-	-
AT3G01790	ribosomal L13 family protein	mtLSU (core)	mtLSU	mtLSU	mitochondrion	+	+	-	-
AT5G46160	50S ribosomal protein (HLP)	mtLSU (core)	mtLSU	mtLSU	mitochondrion	+	+	-	-
AT5G64670	ribosomal L15 family protein	mtLSU (core)	mtLSU	mtLSU	mitochondrion	-	+	-	-
AT4G39880	ribosomal L23 family protein, putative	mtLSU (core)	mtLSU	mtLSU	mitochondrion	-	+	-	-
AT5G23535	50S ribosomal protein L24	mtLSU (core)	mtLSU	mtLSU	mitochondrion	-	+	-	-
AT3G17465	50S ribosomal protein L3-2 (RPL3B)	mtLSU (core)	mtLSU	mtLSU	mitochondrion	-	+	-	-
AT4G31460	ribosomal L28 family protein, putative	mtLSU (core)	other	mtLSU	mitochondrion	-	+	-	-
AT2G37230	rPPR5 (P-class)	mtLSU (core)	other	mtLSU	plastid	-	+	-	-
AT4G28360	ribosomal L22 family protein, putative	mtLSU (core)	other	mtLSU	mitochondrion	-	+	-	-
AT5G40080	ribosomal protein L27 (MRLP27)	mtLSU (pot.)	-	mtLSU	mitochondrion	-	-	-	-
AT1G52370	ribosomal L22 family protein	mtLSU (prob.)	-	mtLSU	mitochondrion	-	+	-	-
AT5G09770	ribosomal L17 family protein, putative	mtLSU (prob.)	mtLSU	mtLSU	mitochondrion	-	+	-	-
AT5G66860	ribosomal L25 family protein /GLN-tRNA synth.	mtLSU (prob.)	mtLSU	mtLSU	mitochondrion	-	+	-	-
AT4G35490	ribosomal protein L11 (MRPL11)	mtLSU (prob.)	mtLSU	mtLSU	mitochondrion	-	+	-	-
AT5G55140	ribosomal L30 family protein	mtLSU (prob.)	mtLSU	mtLSU	mitochondrion	-	+	-	-
AT1G73940	tumor necrosis factor receptor family protein	mtLSU (prob.)	other	mtLSU	mitochondrion	+	+	-	-
AT1G07830	ribosomal L29 family protein	mtLSU (prob.)	other	mtLSU	mitochondrion	-	+	-	-
AT2G20060	50S ribosomal protein L4 (RPL4)	mtLSU (prob.)	other	mtLSU	mitochondrion	-	+	-	-
AT5G49210	stress response NST1-like protein	mtSSU (pot.)	other	unclear	mitochondrion	-	+	-	-

T<small>ABLE</small> I—*continued*

AGI	description	lpBN PAGE (Rugen)	SVC (Rugen)	Waltz	SUBAcon	GFP	MS	cytosolic ribosome	plastid ribosome
2.) components exclusively featured in Waltz et al.									
ATMG00980	ribosomal S12 family protein	-	-	mtSSU	mitochondrion	-	-	-	-
AT2G19720	40S ribosomal protein S15a-2 (RPS15AB)	-	-	mtSSU	cytosol	-	+	+	-
AT1G64600	?	-	-	mtSSU	mitochondrion	-	-	-	-
AT4G21460	ribosomal S24/S35 family protein	-	-	mtSSU	mitochondrion	-	+	-	-
AT4G22000	tyrosine sulfotransferase-like protein	-	other	mtSSU	nucleus	-	-	-	-
AT5G64650	ribosomal L17 family protein	-	-	mtLSU	mitochondrion	-	-	-	-
AT2G16930	50S ribosomal protein L27	-	-	mtLSU	mitochondrion	-	+	-	-
AT5G55125	ribosomal L31 family protein	-	-	mtLSU	mitochondrion	-	-	-	-
AT5G18790	ribosomal L33 family protein, putative	-	-	mtLSU	mitochondrion	-	+	-	-
AT5G20180	ribosomal protein L36	-	-	mtLSU	mitochondrion	-	-	-	-
AT5G39600	39S ribosomal protein	-	-	mtLSU	mitochondrion	-	+	-	-
AT3G01740	ribosomal protein L27 (MRLP27)	-	-	mtLSU	mitochondrion	-	+	-	-
AT2G18400	ribosomal L6 family protein	-	other	mtLSU	mitochondrion	-	+	-	-
AT3G06040	ribosomal L12 family protein, putative	other	other	mtLSU	mitochondrion	-	+	-	-
AT4G37660	ribosomal L12 family protein, putative	other	other	mtLSU	mitochondrion	-	+	-	-
AT1G70190	ribosomal L7/L12 family protein	other	other	mtLSU	mitochondrion	-	+	-	-
AT4G05400	copper ion binding	other	other	mtLSU	mitochondrion	-	+	-	-
AT3G12370	50S ribosomal protein L10	other	mtLSU	mtLSU	mitochondrion	+	+	-	-
AT1G60770	rPPR4 (P-class)	other	mtLSU	mtLSU	mitochondrion	-	+	-	-
AT1G07210	F10K1.8 protein (ribosomal)	other	-	mtSSU	mitochondrion	-	+	-	-
AT5G60960	PNM1/rPPR9 (P-class)	(mtLSU)	mtLSU	mtLSU	mitochondrion	+	+	-	-
AT3G59650	ribosomal L43 family protein, putative	(mtLSU)	mtLSU	mtLSU	mitochondrion	-	+	-	-
AT2G42710	ribosomal L1p/L10e family protein	(mtLSU)	mtLSU	mtLSU	mitochondrion	-	+	-	-
AT2G44065	ribosomal L2 family protein	(mtLSU)	mtLSU	mtLSU	mitochondrion	-	+	-	-
ATMG00210	ribosomal L5 family protein	(mtLSU)	other	mtLSU	mitochondrion	-	+	-	-
AT4G23620	ribosomal L25 family protein /GLN-tRNA synthetase	(mtLSU)	other	mtLSU	mitochondrion	-	+	-	-
AT1G14620	?	(mtLSU)	other	mtLSU	mitochondrion	+	+	-	-
AT5G27820	ribosomal L18p/L5e family protein	(mtLSU)	-	mtLSU	mitochondrion	-	-	-	-
AT1G15810	ribosomal S15 family protein	(mtSSU)	mtSSU	mtSSU	mitochondrion	-	+	-	-
AT4G31810	caseinolytic protease/crotonase family protein (CHY4)	(mtSSU)	mtSSU	mtSSU	mitochondrion	-	+	-	-
AT3G02650	rPPR6 (P-class)	(mtSSU)	mtSSU	mtSSU	mitochondrion	-	+	-	-
AT5G15980	rPPR8 (P-class)	(mtSSU)	mtSSU	mtSSU	mitochondrion	-	+	-	-
3.) components exclusively featured in ribosome clusters from lpBN complexome map of Rugen et al.									
AT1G43170	60S ribosomal protein L3-1 (RPL3A)	mtSSU (pot)	mtLSU	-	cytosol	-	-	+	-
AT5G40405	pentatricopeptide repeat (PPR) protein (DYW-domain)	mtSSU (pot.)	-	-	cytosol	-	-	-	-
AT3G06920	pentatricopeptide repeat (PPR) protein (P-class)	mtSSU (pot.)	-	-	cytosol	-	-	-	-
AT2G34480	60S ribosomal protein L18a-2 (RPL18AB)	mtSSU (pot.)	-	-	cytosol	-	-	+	-
AT1G67430	60S ribosomal protein L17-2 (RPL17B)	mtSSU (pot.)	-	-	cytosol,nucleus	-	-	+	-
AT1G14320	60S ribosomal protein L10-1 (RPL10A)	mtSSU (pot.)	-	-	cytosol	+	-	+	-
AT3G18580	nucleic acid-binding, OB-fold-like protein	mtSSU (pot.)	other	-	mitochondrion	-	+	-	-
AT5G65560	pentatricopeptide repeat (PPR) protein (P-class)	mtSSU (prob)	-	-	mitochondrion	-	+	-	-
AT3G05810	IGR motif protein	mtSSU (prob.)	-	-	mitochondrion	-	-	-	-
AT1G71210	pentatricopeptide repeat (PPR) protein (P-class)	mtSSU (prob.)	other	-	cytosol	-	-	-	-
AT2G31140	peptidase S24/S26A/S26B/S26C fam. Prot. (IMP2)	mtLSU (prob.)	other	-	mitochondrion	-	+	-	-
AT5G54100	stomatin-like protein 2 (SLP2)	mtLSU (prob.)	other	-	mitochondrion	-	+	-	-
AT4G27585	stomatin-like protein 1 (SLP1)	mtLSU (prob.)	other	-	mitochondrion	-	+	-	-
AT2G29080	FtsH protease 3 (FTSH3)	mtLSU (prob.)	other	-	mitochondrion	-	+	-	-
AT1G71260	Whirly 2 (WHY2)	mtLSU (prob.)	other	-	mitochondrion	+	+	-	-
AT1G07510	FtsH protease 10 (FTSH10)	mtLSU (prob.)	other	-	mitochondrion	-	+	-	-
AT1G05430	?	mtLSU (prob.)	other	-	mitochondrion	-	+	-	-
AT1G06200	peptidase S24/S26A/S26B/S26C family protein	mtLSU (prob.)	-	-	cytosol	-	+	-	-
AT3G54980	pentatricopeptide repeat (PPR) protein (P-class)	mtLSU (prob.)	mtLSU	-	mitochondrion	-	+	-	-
AT5G18950	pentatricopeptide repeat (PPR) protein (P-class)	mtLSU (pot.)	-	-	mitochondrion	-	-	-	-
AT4G30700	MEF29 (DYW-domain)	mtLSU (pot.)	-	-	mitochondrion	-	-	-	-
AT4G14850	MEF11 (DYW-domain)	mtLSU (pot.)	-	-	mitochondrion	-	-	-	-
AT2G30780	pentatricopeptide repeat (PPR) protein (P-class)	mtLSU (pot.)	-	-	mitochondrion	-	-	-	-
AT1G76280	pentatricopeptide repeat (PPR) protein (P-class)	mtLSU (pot.)	-	-	mitochondrion	-	+	-	-
AT1G19240	?	mtLSU (pot.)	-	-	peroxisome	-	+	-	-
AT4G11060	organellar single-stranded DNA binding protein 1 (OSB1)	mtLSU (pot.)	other	-	mitochondrion	+	+	-	-
AT3G01910	sulfite oxidase (SOX)	mtLSU (pot.)	other	-	peroxisome	-	+	-	-
AT2G15690	DYW2, (DYW-domain)	mtLSU (pot.)	other	-	mitochondrion	+	-	-	-
AT1G30680	Arabidopsis twinkle homolog (ATH)	mtLSU (pot.)	other	-	mitochondrion	+	+	-	-
ATMG00560	ribosomal L2 family protein	mtLSU (core)	mtLSU	-	mitochondrion	-	+	-	-

Table I—*continued*

AGI	description	lpBN PAGE (Rugen)	SVC (Rugen)	Waltz	SUBAcon	GFP	MS	cytosolic ribosome	plastid ribosome
4.) components exclusively featured in ribosome clusters from sucrose velocity gradient of Rugen et al.									
AT3G55280	60S ribosomal protein L23a-2 (RPL23AB)	-	mtLSU	-	cytosol	-	-	+	-
AT5G60670	60S ribosomal protein L12-3 (RPL12C)	-	mtLSU	-	cytosol	-	-	+	-
AT5G28370	pentatricopeptide repeat (PPR) protein (P-class)	-	mtLSU	-	mitochondrion	-	-	-	-
AT4G05530	short chain dehydrogenase A (SDRA, IBR1)	-	mtLSU	-	peroxisome	-	-	-	-
AT4G29010	abnormal inflorescence meristem 1 (AIM1)	-	mtLSU	-	peroxisome	-	+	-	-
AT3G09630	60S ribosomal protein L4-1 (RPL4A)	-	mtLSU	-	cytosol	-	-	+	-
AT5G62300	40S ribosomal protein S20-1 (RPS20A)	-	mtLSU	-	cytosol	-	+	+	-
AT3G22330	putative mitochondrial RNA helicase 2 (PMH2)	other	mtSSU	-	mitochondrion	-	+	-	-
AT3G15590	pentricopeptide repeat (PPR) protein (P-class)	other	mtSSU	-	mitochondrion	-	+	-	-
AT1G80270	PPR596 (P-class)	other	mtSSU	-	plastid, mitochondrion	+	+	-	-
AT4G35850	pentatricopeptide repeat (PPR) protein (P-class)	other	mtSSU	-	mitochondrion	-	+	-	-
AT5G02740	ribosomal S24e family protein	other	mtSSU	-	mitochondrion	-	+	-	-
AT3G49240	pentatricopeptide repeat (PPR) protein (NUWA, P-class)	other	other	-	mitochondrion	-	+	-	-
AT1G29930	photosystem I/II light harvesting complex SU (LHCB1.3)	contaminant	mtLSU	-	plastid	-	+	-	-
AT2G05070	photosystem II light harvesting complex SU (LHCB2.2)	contaminant	mtLSU	-	plastid	-	-	-	-
AT4G26910	dihydrolipoamide succinyltransferase (OGDCE2)	contaminant	mtLSU	-	mitochondrion	-	+	-	-
AT3G55410	2-oxoglutarate dehydrogenase subunit (OGDCE1)	contaminant	mtLSU	-	mitochondrion	-	+	-	-
AT5G55070	dihydrolipoamide succinyltransferase (OGDCE2)	contaminant	mtLSU	-	mitochondrion	-	+	-	-
AT5G65750	2-oxoglutarate dehydrogenase subunit (OGDCE1)	contaminant	mtLSU	-	mitochondrion	-	+	-	-
AT4G27090	60S ribosomal protein L14-2 (RPL14B)	contaminant	mtLSU	-	cytosol	-	-	+	-
AT3G02490	**pentatricopeptide repeat (PPR) protein (P-class)**	**(mtSSU)**	**mtSSU**	**-**	**mitochondrion**	**-**	**+**	**-**	**-**
AT5G15220	**ribosomal L27 family protein, putative**	**(mtLSU)**	**mtLSU**	**-**	**mitochondrion**	**-**	**-**	**-**	**-**
AT5G16930	**AAA-type ATPase family protein**	**(mtLSU)**	**mtLSU**	**-**	**mitochondrion**	**-**	**+**	**-**	**-**

AGI, Arabidopsis genome identifier; description, functional/structural protein annotation; lpBN PAGE (Rugen), subunit affiliation according to lpBN complexome map; SVC (Rugen), subunit affiliation according to sucrose velocity gradient complexome map; Waltz, subunit affiliation according to Waltz et al. (57); SUBAcon, subcellular location according to the SUBAcon algorithm (49); GFP, experimental evidence for mitochondrial location according to fluorescent fusion reporter protein assay; MS, experimental evidence for mitochondrial location according to MS analysis of isolated organelles; cytosolic ribosome, detection of AGI in isolated cytosolic ribosomes according to (56); plastid ribosome, detection of AGI in isolated cytosolic ribosomes according to (78). Rows shown in red indicate diverging LSU/SSU assignments; bold rows are expected to be genuine mitoribosomal proteins; rows shown in bold and italics indicate additional units potentially affiliated with mitoribosomes; subunit assignments shown in brackets indicate the absence of proteins from the subunit cluster but a local peak in either the mtSSU or mtLSU in the heatmap of cross-linked leaf mitochondria (supplemental Fig. S11); peach, mtSSU; light blue, mtLSU.

potential mtSSU components, four of which (AT2G34480, AT1G67430, AT1G14320, and AT1G43170) have annotations identifying them as eukaryotic LSU proteins. These proteins were also identified in an investigation of Arabidopsis cytosolic ribosomes (56). Although clustering with the mtSSU proteins, they show minor differences in their migration pattern and should not be regarded as mitochondrial SSU subunits. Their incorporation into the SSU cluster is more likely the result of co-migration of cytosolic LSU subunits with mtSSU subunits. Two other potential mtSSU proteins are a nucleic acid binding protein (AT3G18580) and an IGR motif carrying protein of unknown function. Their potential functions in mitochondrial translation are currently unknown.

Twenty potential mitoribosomal proteins being featured in our mtLSU cluster were not found by Waltz et al. (57). Of these, only one belongs to the core cluster (ATMG00560) and is annotated as a ribosomal L2 family protein. The remaining 19 proteins belong in equal parts to the probable and potential classes of LSU proteins. Six members of the LSU cluster are related to protein fate: FtsH3 and 10 (AT2G29080, AT1G07510), stomatin-like proteins 1 and 2 (SLP1/2; AT5G54100, AT4G27585), and two members of the S24/S26 peptidase family (AT2G31140, AT1G06200). FtsH3 and FtsH10 are AAA-proteases and, together with prohibitins, they form homo- and hetero-oligomeric complexes of ~2 MDa (58). In our hands, no direct correlation between FtsH3/10 and prohibitins could be detected. However, besides their main peak at ~1.1 MDa, prohibitins possess a second, minor peak close to the FtsH peak (Suppl. Fig. 11). Interestingly, the precursor polypeptide chain of RPL32 is trimmed by FtsH to yield the mature protein. RPL32 (AT1G26740) has not been identified by Waltz et al. (57), nor by us. It is, however, predicted to be located in mitochondria, and double knock-out mutants of FtsH3 and FtsH10 show reduced rates of mitochondrial gene expression rates (59). Hence, a potential functional connection between FtsH proteins and ribosomal proteins exists and strengthens the notion of a physical connection of these proteins. SLP, together with prohibitins belong to the band-7 family which is also referred to as SPFH superfamily. Detailed functions for the members of this protein family are unknown but seem to revolve around protein scaffolding and organization of the inner mitochondrial membrane (60). Murine SLP2 co-migrates with the mtLSU in

sucrose velocity gradients, and the protein was identified as being a key regulator of mitochondrial translation in mice (61). Hence, the presence of these proteins in the mtLSU cluster is backed by a connection to translation. No such connection between the S24/S26 peptidases and mitochondrial translation could be found. Other proteins which are found here but are missing in Waltz *et al.* (57) include two proteins of unknown function (AT1G05430, AT1G19240), an organellar single stranded DNA binding protein (AT4G11060), and an Arabidopsis twinkle homolog (AT1G30680), both of which have implicated roles in mtDNA replication (62), Whirly 2 (AT1G71260, potentially involved in DNA maturation), as well as a sulfite oxidase (AT3G01910). The remaining seven proteins are either cytosolic ribosomal subunits or PPR proteins (see below). Taken together, the proteins involved in protein maturation featured in the LSU cluster may indeed have functions in translation. Given their absence in the dataset of Waltz *et al.* (57), we speculate that they form an additional loosely bound unit which is most likely located in the inner mitochondrial membrane. Due to the cross-linking strategy employing formaldehyde, it co-migrates with the mtLSU in lpBN-PAGE. Formaldehyde has been used here in moderation and the distance it can bridge is small compared with other cross-linkers. The tendency to produce artificial protein aggregates is therefore rather small. Considering that many protein complexes, for example of the respiratory chain, remain unchanged upon its use, the additional proteins detected in the LSU and SSU clusters in the lpBN-based complexome map cannot be attributed solely to the use of formaldehyde; rather they represent candidates for ribosome members.

From the data of Waltz *et al.* (57), the heatmaps shown here, and subcellular information as well as additional information available from TAIR (Arabidopsis.org), a set of 92 proteins was extracted which constitutes the essence of the Arabidopsis mitoribosome (bold rows in Table 1). Within this set, 42 proteins are in the mtSSU, 48 in the mtLSU, and two additional proteins could not clearly be assigned to either one.

The Presence of PPR-proteins In the Ribosomal Fractions—Together, mitochondria and plastids contain several hundreds of PPR proteins. For many of them, no functional context has been identified. However, a considerable number of PPR proteins are involved in RNA processing (63). The presence of PPR-proteins has been linked to the ribosomes of plastids and mitochondria (22, 64–66) and 20 PPRs have been identified in the mtSSU and mtLSU clusters of the lpBN based complexome map or by Waltz *et al.* (57). Six of these were found in both studies, with the PPR protein used in Waltz *et al.* (57) for immune-precipitation of mitoribosomes, PPR336 (rPPR1, P-class), being among them. The remaining five PPR proteins are also members of the P-class of PPR proteins. Four PPR proteins were exclusively found by Waltz *et al.* (57) and belong to the P-class of PPR proteins. In contrast, ten PPR were exclusively identified here, of which six belong to the P-class. The other four are members of the PLS-class and

contain DYW-domains (AT2G15690, DYW2; AT4G14580, MEF11; AT4G30700, MEF29; AT5G40405, unknown function; Table 1). DWY2 provides the deaminase activity to a suggested editosome protein complex, which also contains NUWA and SLO2 (67). NUWA was detected in the lpBN as well as in the sucrose velocity gradient complexome maps but did not cluster with the ribsosomal proteins. Its abundance profiles, however, show weak local highs in the area of the mtSSU clusters (please see the extra rows inserted into the heatmaps shown in Figs. 3 and 5). SLO2 was not discovered in either of the two approaches. Among the remaining three PLS-type PPR proteins are two mitochondrial editing factors (MEFs), MEF11 and MEF29. MEF11 is involved in editing three mitochondrial transcripts for respiratory chain subunits (*cox3, nad4, and ccb*), while MEF29 is required for editing respiratory protein complex subunits *nad5* and *cob* (68, 69). Information of the fourth PLS-type PPR (AT5G40405.1) is scarce and no comment on its potential functions as part of the mitoribosome can be made. The presence of these DYW-domain containing PPR proteins in the ribosomal clusters suggest a physical connection between RNA editing and translation in plant mitochondria. Analogous to the situation described for the FtsH/SLP/S-peptidase cluster described above, the presence of these mRNA editing factors within our heatmap may be due to a cross-linking event between an RNA-editing unit and the ribosome. Given that the migration pattern differs between AT5G40405 (in the SSU cluster) and MEF29, MEF11, and DYW2 (all of them in the LSU cluster), this extra subunit may be attached to both subunits. Little is known about the residual 16 PPR proteins belonging to the P-class, but some of them enhance translational activity for specific proteins (reviewed in (63)). Three P-class PPRs, however were found to interact with ribosomes/polyribosomes (PPR336, PPR 596, and PNM1; (22, 66). As such, the other P-class PPRs identified in the course of this study may also be at least temporary members of Arabidopsis mitoribosomal subunits.

Molecular Masses of mtSSU and mtLSU Clusters—The masses for the mtLSU cluster members (proteins of all three confidence intervals and 5S/26S rRNA) amount to a mass of 2.7 MDa, which is close to the apparent molecular mass of 3 MDa. However, the bulk of the abundance of the core proteins is distributed over four fractions and for most proteins the overall width of the cluster stretches over seven to nine fractions and is thus broader than the mtLSU cluster. The width of a cluster in a complexome heatmap is determined in some part by the fractionation of the gel lane and may therefore vary between replicates. However, we observed the same outcome for the mtLSU cluster repeatedly in heatmaps of cross-linked leaf mitochondria (data not shown). As such, the width of the cluster is most likely a result of some variation in molecular mass and, therefore in the composition of the mtLSU. Not all proteins of the mtLSU cluster may be present within the same large subunit at a given time point.
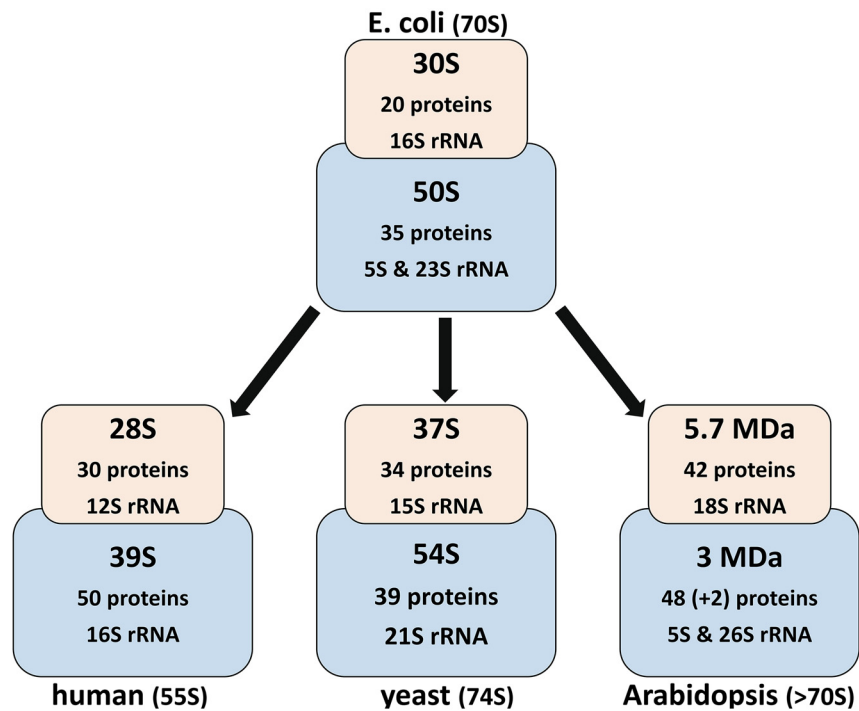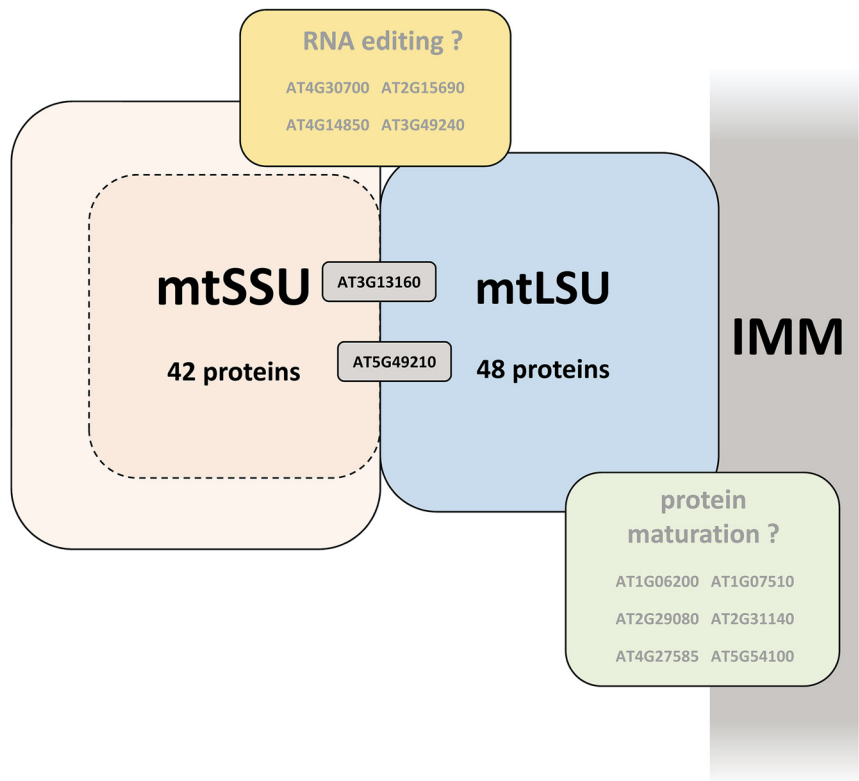
FIG. 6. **Composition of bacterial and mitochondrial RPL and RPS clusters.** *A,* general overview of the composition of LSU and SSU of *E. coli* ribosomes with that of the mtLSUs and mtSSUs of yeast (8, 10, 11) and humans (12–15), as well as the provisional Arabidopsis mtLSU and mtSSU (as deduced from the data presented by Waltz *et al.* (57) and here). *B,* the Arabidopsis mtSSU and mtLSU together with potential additional units involved in RNA editing (yellow) and protein maturation (green). The Arabidopsis mtSSU appears to be larger than the LSU, the underlying reason for this is a matter of debate. Accessions in gray boxes indicate proteins for which assignment to either of the two subunits is not clear. Peach, (mt)SSU; light blue (mt)LSU; IMM, inner mitochondrial membrane.

Intriguingly, the masses of the precursor proteins in the mtSSU cluster accumulate to ~1.6 MDa. Together with the 18S RNA, this results in a mass of ~2.2 MDa for the small subunit. Hence, its calculated mass is less than half of the apparent mass of 5.7 MDa. Waltz *et al.* (57) speculate that the high mass of the mtSSU is inflicted by the presence of additional (PPR) proteins as well as additional mRNA loops. Given that the overlap between the two studies is high for the SSU (33 proteins of 41 reported by Waltz *et al.* (57) and of 38 reported here), this may partly explain the mass difference between the plant mtSSU and the prokaryotic SSU. However, since the additional mtSSU components are already considered in our calculations, the bulk of difference between apparent and calculated mass of the ribosomes must be due to other factors. One such factor could be the shape of the particle, which may affect its electrophoretic mobility. Despite a similar molecular mass, a globular particle will face less resistance to migration in a polyacrylamide gel than an irregularly shaped particle with protrusions. MtSSU particles of the latter type have been described by Waltz *et al.* (57). Another requirement for the migration in a gel is a net negative charge, which is conferred to the complexes by a coat of the negatively charged protein dye Coomassie (70). This Coomassie-coating, however, may also impact on protein complexes in unknown ways and may thus affect their separation in the gel matrix. Both, shape and Coomassie coat, can be ruled out as major factors influencing the apparent molecular mass of the mtSSU since the sucrose velocity gradient confirms the results obtained from the lpBN gel. Alternatively, the association of the ribosomes with the inner mitochondrial membrane may affect the molecular mass of the ribosomes since lipids may remain attached to the particles upon solubilization. This, however, is unlikely since interaction of the ribosome with the membrane will most likely take place at the mtLSU surface and therefore will have little impact on the mass of the mtSSU. Instead, the apparent mass may suggest the presence of mtSSU dimers. In bacteria, inactive (hibernating) ribosomes are "stored" as dimers (100S ribosomes), the contact side of the two monomers being conferred by the SSU (71–77). As mitochondria have their origin in the bacterial kingdom, the mtSSU observed here may represent dimeric mitochondrial ribosomes which are lacking the two mtLSUs. Indeed, Waltz *et al.* (57) observed aggregation of ribosomal subunits in sucrose velocity gradients. However, dimerization of bacterial 70S ribosomes requires the presence of a ribosome modulation factor (RMF) protein and/or a hibernation promoting factor (HPF) protein, but no homologues for such proteins were found in the lpBN-based or the sucrose velocity gradient-based mitochondrial heatmaps. Further analysis of mtSSU particles, for example by crosslinking MS or cryo-EM, will be necessary to elucidate the source of the additional mass of the Arabidopsis mtSSU.

CONCLUSIONS

The data presented here shed new light on the protein composition of plant mitoribosomes. Using a combination of chemical cross-linking and complexome profiling employing both, lpBN gel electrophoresis and sucrose velocity gradients, mitoribosomal proteins were identified on a large scale. Since the ribosomal subunits were separated by this approach, the data allow a clear allocation of proteins to either the large or the small subunit. In conjunction with a recently published study using different experimental approaches, a set of 92 proteins was assembled which most likely constitute Arabidopsis mitoribosomes (Table 1). Compared with its bacterial ancestor and the mammalian as well as fungal mitoribosomes, plant mitoribosomes are thus believed to contain the highest total number of proteins (Fig. 6*A*). This is because each subunit contains non-conventional proteins, most of which belong to the PPR-class. The functions of most of these proteins in the context of translation are just beginning to emerge. However, the presence of several PPR-proteins containing DYW domains suggests that RNA editing may to some degree occur at mitochondrial ribosomes. Furthermore, proteins involved in protein maturation and protein degradation were also detected as potential components of the large subunit and may play a role in processing nascent polypeptides (Table 1, Fig. 6*B*). Remarkably, the data presented here imply an unusual molecular mass of the small ribosomal subunit, which is higher than that of the large subunit and only partly explainable by the presence of additional, plant specific components. Future efforts are necessary to investigate the roles of the newly identified, non-conventional subunits as well as the origin of the high molecular mass of the small mitoribosomal subunit.

DATA AVAILABILITY

The mass spectrometry proteomics data have been deposited to the ProteomeXchange Consortium via the PRIDE partner repository with the dataset identifier PXD011088 (http://www.ebi.ac.uk/pride/archive/projects/PXD011088; ftp://ftp.pride.ebi.ac.uk/pride/data/archive/2019/04/PXD011088).

REFERENCES

1. Kubo, T., and Newton, K. J. (2008) Angiosperm mitochondrial genomes and mutations. *Mitochondrion* **8,** 5–14

2. Hamilton, M. G., and O'Brien, T. W. (1974) Ultracentrifugal characterization of the mitochondrial ribosome and subribosomal particles of bovine liver: molecular size and composition. *Biochemistry* **13,** 5400–5403

3. Zhang, Y., and Spremulli, L. L. (1998) Roles of residues in mammalian mitochondrial elongation factor Ts in the interaction with mitochondrial and bacterial elongation factor Tu. *J. Biol Chem.* **273,** 28142–28148

4. Gaur, R., Grasso, D., Datta, P. P., Krishna, P. D., Das, G., Spencer, A., Agrawal, R. K., Spremulli, L., and Varshney, U. (2008) A single mammalian mitochondrial translation initiation factor functionally replaces two bacterial factors. *Mol. Cell* **29,** 180–190

5. Desmond, E., Brochier-Armanet, C., Forterre, P., and Gribaldo, S. (2011) On the last common ancestor and early evolution of eukaryotes: reconstructing the history of mitochondrial ribosomes. *Res. Microbiol.* **162,** 53–70

6. Brown, A., Amunts, A., Bai, X. C., Sugimoto, Y., Edwards, P. C., Murshudov, G., Scheres, S. H. W., and Ramakrishnan, V. (2014) Structure of the large ribosomal subunit from human mitochondria. *Science* **346,** 718–722

7. Amunts, A., Brown, A., Toots, J., Scheres, S. H. W., and Ramakrishnan, V. (2015) Ribosome. The structure of the human mitochondrial ribosome. *Science* **348,** 95–98

8. Desai, N., Brown, A., Amunts, A., and Ramakrishnan, V. (2017) The structure of the yeast mitochondrial ribosome. *Science* **355,** 528–531

9. Ramrath, D. J. F., Niemann, M., Leibundgut, M., Bieri, P., Prange, C., Horn, E. K., Leitner, A., Boehringer, D., Schneider, A., and Ban, N. (2018) Evolutionary shift toward protein-based architecture in trypanosomal mitochondrial ribosomes. *Science* **362,** eaau7735

10. Amunts, A., Brown, A., Bai, X. C., Llácer, J. L., Hussain, T., Emsley, P., Long, F., Murshudov, G., Scheres, S. H. W., and Ramakrishnan, V. (2014) Structure of the yeast mitochondrial large ribosomal subunit. *Science* **343,** 1485–1489

11. Greber, B. J., and Ban Structure, N. (2016) Function of the mitochondrial ribosome. *Annu. Rev. Biochem.* **85,** 103–132

12. O'Brien, T. W. (1971) The general occurrence of 55 S ribosomes in mammalian liver mitochondria. *J. Biol. Chem.* **246,** 3409–3417

13. Cahill, A., Baio, D. L., and Cunningham, C. C. (1995) Isolation and Characterization of rat liver mitochondrial ribosomes. *Anal. Biochem.* **232,** 47–55

14. Amunts, A., Brown, A., Toots, J., Scheres, S. H. W., and Ramakrishnan, V. (2015) The structure of the human mitochondrial ribosome. *Science* **348,** 95–98

15. Greber, B. J., Bieri, P., Leibundgut, M., Leitner, A., Aebersold, R., Boehringer, D., and Ban, N. (2015) The complete structure of the 55S mammalian mitochondrial ribosome. *Science* **348,** 303–308

16. Liu, M., and Spremulli, L. (2000) Interaction of mammalian mitochondrial ribosomes with the inner membrane. *J. Biol. Chem.* **275,** 29400–29406

17. Pfeffer, S., Woellhaf, M. W., Herrmann, J. M., and Forster, F. (2015) Organization of the mitochondrial translation machinery studied in situ by cryoelectron tomography. *Nat. Commun.* **6,** 6019

18. Greber, B. J., Boehringer, D., Leibundgut, M., Bieri, P., Leitner, A., Schmitz, N., Aebersold, R., and Ban, N. (2014) The complete structure of the large subunit of the mammalian mitochondrial ribosome. *Nature* **515,** 283–286

19. Sharma, M. R., Koc, E. C., Datta, P. P., Booth, T. M., Spremulli, L. L., and Agrawal, R. K. (2003) Structure of the mammalian mitochondrial ribosome reveals an expanded functional role for its component proteins. *Cell* **115,** 97–108

20. Greber, B. J., Boehringer, D., Leitner, A., Bieri, P., Voigts-Hoffmann, F., Erzberger, J. P., Leibundgut, M., Aebersold, R., and Ban, N. (2014) Architecture of the large subunit of the mammalian mitochondrial ribosome. *Nature* **505,** 515–519

21. Lurin, C., Andrés, C., Aubourg, S., Bellaoui, M., Bitton, F., Bruyère, C., Caboche, M., Debast, C., Gualberto, J., Hoffmann, B., Lecharny, A., Le Ret, M., Martin-Magniette, M. L., Mireau, H., Peeters, N., Renou, J. P., Szurek, B., Taconnat, L., and Small, l. (2004) Genome-wide analysis of Arabidopsis pentatricopeptide repeat proteins reveals their essential role in organelle biogenesis. *Plant Cell* **16,** 2089–2103

22. Uyttewaal, M., Mireau, H., Rurek, M., Hammani, K., Arnal, N., Quadrado, M., and Giegé, P. (2008) PPR336 is associated with polysomes in plant mitochondria. *Mol. J. Biol.* **375,** 626–636

23. Leaver, C. J., and Harmey, M. A. (1973) Plant mitochondrial nucleic acids. *Biochem. Soc. Symposia* **38,** 175–193

24. Vasconcelos, A. C., and Bogorad, L. (1971) Proteins of cytoplasmic, chloroplast, and mitochondrial ribosomes of some plants. *Biochim. Biophys. Acta* **228,** 492–502

25. Pinel, C., Douce, R., and Mache, R. (1986) A study of mitochondrial ribosomes from the higher plant Solanum tuberosum L. *Mol. Biol. Reports* **11,** 93–97

26. Maffey, L., Degand, H., and Boutry, M. (1997) Partial purification of mitochondrial ribosomes from broad bean and identification of proteins encoded by the mitochondrial genome. *Mol. General Gen.* **254,** 365–371

27. Heazlewood, J. L., Tonti-Filippini, J. S., Gout, A. M., Day, D. A., Whelan, J., and Millar, A. H. (2004) Experimental analysis of the Arabidopsis mitochondrial proteome highlights signaling and regulatory components, provides assessment of targeting prediction programs, and indicates plant-specific mitochondrial proteins. *Plant Cell* **16,** 241–256

28. Huang, S., Taylor, N. L., Narsai, R., Eubel, H., Whelan, J., and Millar, A. H. (2009) Experimental analysis of the rice mitochondrial proteome, its biogenesis, and heterogeneity. *Plant Physiol.* **149,** 719–734

29. Klodmann, J., Senkler, M., Rode, C., and Braun, H. P. (2011) Defining the protein complex proteome of plant mitochondria. *Plant Physiology* **157,** 587–598

30. Salvato, F., Havelund, J. F., Chen, M., Rao, R. S., Rogowska-Wrzesinska, A., Jensen, O. N., Gang, D. R., Thelen, J. J., and Møller, I. M. (2014) The potato tuber mitochondrial proteome. *Plant Physiol.* **164,** 637–653

31. Senkler, J., Senkler, M., Eubel, H., Hildebrandt, T., Lengwenus, C., Schertl, P., Schwarzländer, M., Wagner, S., Wittig, I., and Braun, H. P. (2017) The mitochondrial complexome of Arabidopsis thaliana. *Plant J.* **89,** 1079–1092

32. Wegrzyn, R. D., and Deuerling, E. (2005) Molecular guardians for newborn proteins: ribosome-associated chaperones and their role in protein folding. *Cell. Mol. Life Sci.* **62,** 2727–2738

33. Pfeffer, S., Woellhaf, M. W., Herrmann, J. M., and Förster, F. (2015) Organization of the mitochondrial translation machinery studied in situ by cryoelectron tomography. *Nature Commun.* **6,** 6019

34. Heide, H., Bleier, L., Steger, M., Ackermann, J., Dröse, S., Schwamb, B., Zörnig, M., Reichert, A. S., Koch, I., Wittig, I., and Brandt, U. (2012) Complexome profiling identifies TMEM126B as a component of the mitochondrial complex I assembly complex. *Cell Metabolism* **16,** 538–549

35. Strecker, V., Wumaier, Z., Wittig, I., and Schägger, H. (2010) Large pore gels to separate mega protein complexes larger than 10 MDa by blue native electrophoresis: isolation of putative respiratory strings or patches. *Proteomics* **10,** 3379–3387

36. Cavalcanti, J. H. F., Quinhones, C. G. S., Schertl, P., Brito, D. S., Eubel, H., Hildebrandt, T., Nunes-Nesi, A., Braun, H. P., and Araújo, W. L. (2017) Differential impact of amino acids on OXPHOS system activity following carbohydrate starvation in Arabidopsis cell suspensions. *Physiologia Plantarum* **161,** 451–467

37. Thal, B., Braun, H. P., and Eubel, H. (2018) Proteomic analysis dissects the impact of nodulation and biological nitrogen fixation on Vicia faba root nodule physiology. *Plant Mol. Biol.* **97,** 233–251

38. Cox, J., and Mann, M. (2008) MaxQuant enables high peptide identification rates, individualized p.p.b.-range mass accuracies and proteome-wide protein quantification. *Nat. Biotechnol.* **26,** 1367–1372

39. Schwanhäusser, B., Busse, D., Li, N., Dittmar, G., Schuchhardt, J., Wolf, J., Chen, W., and Selbach, M. (2011) Global quantification of mammalian gene expression control. *Nature* **473,** 337–342

40. Giese, H., Ackermann, J., Heide, H., Bleier, L., Dröse, S., Wittig, I., Brandt, U, and Koch, I. (2015) NOVA: a software to analyze complexome profiling data. *Bioinformatics* **31,** 440–441

41. Liu, X., Yang W. C., Gao, Q, and Regnier, F. (2008) Toward chromatographic analysis of interacting protein networks. *J. Chromatography* **1178,** 24–32

42. Kirkwood, K. J., Ahmad, Y., Larance, M., and Lamond, A. I. (2013) Characterization of native protein complexes and protein isoform variation using size-fractionation-based quantitative proteomics. *Mol. Cell. Proteomics* **12,** 3851–3873

43. Wan, C., Borgeson, B., Phanse, S., Tu F., Drew, K., Clark, G., Xiong, X., Kagan, O., Kwan, J., Bezginov, A., Chessman, K., Pal S., Cromar, G., Papoulas, O., Ni, Z., Boutz, D. R., Stoilova, S., Havugimana, P. C., Guo, X., Malty, R. H., Sarov, M., Greenblatt, J., Babu, M., Derry, W. B., Tillier,

E. R., Wallingford, J. B., Parkinson, J., Marcotte, E. M., and Emili, A. (2015) Panorama of ancient metazoan macromolecular complexes. *Nature* **525,** 339–344

44. Olinares, P. D. B., Ponnala, L., and van Wijk, K. J. (2010) Megadalton complexes in the chloroplast stroma of Arabidopsis thaliana characterized by size exclusion chromatography, mass spectrometry, and hierarchical clustering. *Mol. Cell. Proteomics* **9,** 1594–1615

45. Aryal, U. K., Xiong, Y., McBride, Z., Kihara, D., Xie, J., Hall, M. C., and Szymanski, D. B. (2014) A proteomic strategy for global analysis of plant protein complexes. *Plant Cell* **26,** 3867–3882

46. Aryal, U. K., McBride, Z., Chen, D., Xie, J., and Szymanski, D. B. (2017) Analysis of protein complexes in Arabidopsis leaves using size exclusion chromatography and label-free protein correlation profiling. *J. Proteomics* **166,** 8–18

47. McBride, Z., Chen, D., Reick, C., Xie, J., and Szymanski, D. B. (2017) Global analysis of membrane-associated protein oligomerization using protein correlation profiling. *Mol. Cell. Proteomics* **16,** 1972–1989

48. Cox, J., and Mann, M. (2008) MaxQuant enables high peptide identification rates, individualized p.p.b.-range mass accuracies and proteome-wide protein quantification. *Nature Biotechnol.* **26,** 1367–1372

49. Hooper, C. M., Tanz, S. K., Castleden, I. R., Vacher, M. A., Small, I. D., and Millar, A. H. (2014) SUBAcon: a consensus algorithm for unifying the subcellular localization data of the Arabidopsis proteome. *Bioinformatics* **30,** 3356–3364

50. Braun, H. P., Binder, S., Brennicke, A., Eubel, H., Fernie, A. R., Finkemeier, I., Klodmann, J., König, A. C., Kühn, K, Meyer, E., Obata, T., Schwarzländer, M., Takenaka, M., and Zehrmann, A. (2014) The life of plant mitochondrial complex I. *Mitochondrion* **19,** 295–313

51. Eubel, H., Jänsch, L., and Braun, H. P. (2003) New insights into the respiratory chain of plant mitochondria. Supercomplexes and a unique composition of complex II. *Plant Physiol.* **133,** 274–286

52. Patel, M. S., Nemeria, N. S., Furey, W., and Jordan, F. (2014) The pyruvate dehydrogenase complexes: structure-based function and regulation. *J. Biol. Chem.* **289,** 16615–16623

53. Bonen, L., and Calixte, S. (2006) Comparative analysis of bacterial-origin genes for plant mitochondrial ribosomal proteins. *Mol. Biol. Evolution* **23,** 701–712

54. Carroll, A. J., Heazlewood, J. L., Ito, J., and Millar, A. H. (2008) Analysis of the Arabidopsis cytosolic ribosome proteome provides detailed insights into its components and their post-translational modification. *Mol. Cell. Proteomics* **7,** 347–369

55. Suissa, M., and Schatz, G. (1982) Import of proteins into mitochondria. Translatable mRNAs for imported mitochondrial proteins are present in free as well as mitochondria-bound cytoplasmic polysomes. *J. Biol. Chem.* **257,** 13048–13055

56. Hummel, M., Dobrenel, T., Cordewener, J. J., Davanture, M., Meyer, C., Smeekens, S. J., Bailey-Serres, J., America, T. A., and Hanson, J. (2015) Proteomic LC-MS analysis of Arabidopsis cytosolic ribosomes: Identification of ribosomal protein paralogs and re-annotation of the ribosomal protein genes. *J. Proteomics* **128,** 436–449

57. Waltz, F., Nguyen, T. T., Arrivé, M., Bochler, A., Chicher, J., Hammann, P., Kuhn, L., Quadrado, M., Mireau, H., Hashem, Y., and Giegé, P. (2019) Small is big in Arabidopsis mitochondrial ribosome. *Nature Plants* **5,** 106–117

58. Piechota, J., Kolodziejczak, M., Juszczak, I., Sakamoto, W., and Janska, H. (2010) Identification and characterization of high molecular weight complexes formed by matrix AAA proteases and prohibitins in mitochondria of Arabidopsis thaliana. *J. Biol. Chem.* **285,** 12512–12521

59. Kolodziejczak, M., Skibior-Blaszczyk, R., and Janska, H. (2018) m-AAA complexes are not crucial for the survival of Arabidopsis under optimal growth conditions despite their importance for mitochondrial translation. *Plant Cell Physiol.* **59,** 1006–1016

60. Gehl, B., Lee, C. P., Bota, P., Blatt, M. R., and Sweetlove, L. J. (2014) An Arabidopsis stomatin-like protein affects mitochondrial respiratory supercomplex organization. *Plant Physiol.* **164,** 1389–1400

61. Mitsopoulos, P., Lapohos, O., Weraarpachai, W., Antonicka, H., Chang, Y. H., and Madrenas, J. (2017) Stomatin-like protein 2 deficiency results in impaired mitochondrial translation. *PloS One* **12,** e0179967

62. Zaegel, V., Guermann, B., Le Ret, M., Andrés, C., Meyer, D., Erhardt, M., Canaday, J., Gualberto, J. M., and Imbault, P. (2006) The plant-specific ssDNA binding protein OSB1 is involved in the stoichiometric transmission of mitochondrial DNA in Arabidopsis. *Plant Cell* **18,** 3548–3563

63. Barkan, A., and Small, I. (2014) Pentatricopeptide repeat proteins in plants. *Ann. Rev. Plant Biol.* **65,** 415–442

64. Williams, P. M., and Barkan, A. (2003) A chloroplast-localized PPR protein required for plastid ribosome accumulation. *Plant J.* **36,** 675–686

65. Aphasizheva, I., Maslov, D. A., Qian, Y., Huang, L., Wang, Q., Costello, C. E., and Aphasizhev, R. (2016) Ribosome-associated pentatricopeptide repeat proteins function as translational activators in mitochondria of trypanosomes. *Mol. Microbiol.* **99,** 1043–1058

66. Hammani, K., Gobert, A., Hleibieh, K., Choulier, L., Small, I., and Giegé, P. (2011) An Arabidopsis dual-localized pentatricopeptide repeat protein interacts with nuclear proteins involved in gene expression regulation. *Plant Cell* **23,** 730–740

67. Andrés-Colás N., Zhu, Q., Takenaka, M., De Rybel, B., Weijers, D., and Van Der Straeten, D. (2017) Multiple PPR protein interactions are involved in the RNA editing system in Arabidopsis mitochondria and plastids. *Proc. Natl. Acad. Sci. U.S.A.* **114,** 8883–8888

68. Verbitskiy, D., Zehrmann, A., Brennicke, A., and Takenaka, M. (2010) A truncated MEF11 protein shows site-specific effects on mitochondrial RNA editing. *Plant Signaling Behavior* **5,** 558–560

69. Sosso, D., Mbelo, S., Vernoud, V., Gendrot, G., Dedieu, A., Chambrier, P., Dauzat, M., Heurtevin, L., Guyon, V., Takenaka, M., and Rogowsky, P. M. (2012) PPR2263, a DYW-subgroup pentatricopeptide repeat protein is required for mitochondrial nad5 and cob transcript editing mitochondrion biogenesis and maize growth. *Plant Cell* **24,** 676–691

70. Schägger, H., and von Jagow, G. (1991) Blue native electrophoresis for isolation of membrane protein complexes in enzymatically active form. *Anal. Biochem.* **199,** 223–231

71. Yoshida, H., Maki, Y., Kato, H., Fujisawa, H., Izutsu, K., Wada, C., and Wada, A. (2002) The ribosome modulation factor (RMF) binding site on the 100S ribosome of Escherichia coli. *J. Biochem.* **132,** 983–989

72. Beckert, B., Turk, M., Czech, A., Berninghausen, O., Beckmann, R., Ignatova, Z., Plitzko, J. M., and Wilson, D. N. (2018) Structure of a hibernating 100S ribosome reveals an inactive conformation of the ribosomal protein S1. Nat. Microbiol. **3,** 1115–1121

73. Ueta, M., Ohniwa, R. L., Yoshida, H., Maki, Y., Wada, C., and Wada, A. (2008) Role of HPF (hibernation promoting factor) in translational activity in Escherichia coli. *J. Biochem.* **143,** 425–433

74. Franken, L. E., Oostergetel, G. T., Pijning, T., Puri, P., Arkhipova, V., Boekema, E.J., Poolman, B., and Guskov, A. (2017) A general mechanism of ribosome dimerization revealed by single-particle cryo-electron microscopy. *Nat. Commun.* **8,** 722

75. Trösch, R., and Willmund, F. (2019) The conserved theme of ribosome hibernation: from bacteria to chloroplasts of plants. *Biol. Chem.* 10.1515/hsz-2018-0436

76. Huxley, H. E., and Zubay, G. (1960) Electron microscope observations on the structure of microsomal particles from Escherichia coli. *J. Mol. Biol.* **2,** 10-IN8

77. Matzov, D., Aibara, S., Basu, A., Zimmerman, E., Bashan, A., Yap, M. N. F., Amunts, A., and Yonath, A. E. (2017) The cryo-EM structure of hibernating 100S ribosome dimer from pathogenic Staphylococcus aureus. *Nat. Comm.* **8,** 723

78. Tiller, N., and Bock, R. (2014) The translational apparatus of plastids and its role in plant development. *Mol. Plant* **7,** 1105–1120